CHAPTER V
RESULTS

1. Screening of a cDNA library with a legumain conserved probe and analysis of sequences of FgLGMN-1 and FgLGMN-2 isolated from a cDNA library of adult *Fasciola gigantica*

1.1 PCR amplification and cloning of recombinant FgLGMNs

Fasciola gigantica asparaginyl endopeptidase or legumain (LGMN) cDNAs were amplified by PCR with degenerated primers from an adult stage *F. gigantica* cDNA library. The primers were designed based on the highly conserved regions of the legumain family by using the information of related orthologs that are available in the GenBank database. The PCR products were size-separated in a 1% agarose gel and their correct size was proven by comparison with a 1 kb DNA ladder size standard. The PCR product was obtained with the estimated sizes of approximately 317 bp. The PCR product was extracted from the agarose gel and ligated to the pGEM®-T Easy cloning vector. *E. coli* XL1-Blue cells were transformed with the ligation products and the success of transformation was tested by PCR and restriction endonucleases analysis with *Eco*R I. The PCR product and digested plasmid DNA showed inserts of the correct size. The digested fragment was subjected to prepare radioactive labeled DNA probes and used for cDNA library screening.

1.2 cDNA library screening for full-length FgLGMNs

Full-length asparaginyl endopeptidase or legumain (LGMN) cDNAs were screened in an adult stage *F. gigantica* cDNA library (high density: 5×10^4 pfu/ml) with a radioactive labeled DNA probe that was specific to a highly conserved region of the legumain family. After autoradiography, several positive plaques were detected on the hybridized membranes (Figure 8). Several positive plaques were obtained and phages were eluted for re-infection of host bacteria for plaque formation (low density). The low density plates were screened again to isolate single well-isolated plaques. The positives plaques were obtained to isolate λTriplEx2 phages carrying specific

cDNAs and used to infect BM25.8 strain *E. coli* containing the helper phage that was available for single-clone excision to pTriplEx2 phagemids. pTriplEx2 were isolated and the size of inserted fragments was determined by digestion with *Kpn* I and *Xho* I restriction endonucleases and then analyzed by 1% agarose gel electrophoresis. Ten clones containing the longest cDNA fragments were analyzed by nucleic acid sequencing.

1.3 Nucleic acid sequences analysis

The nucleotide sequences showed that two different types of full-length cDNA were isolated. Electrophoresis analysis of digested recombinant plasmid with *Kpn* I and *Xho* I restriction endonucleases showed isoform-1 of approximately 1,400 bp (Figure 9A) and of isoform-2 of approximately 1,350 bp (Figure 9B). Analysis of nucleotide sequences revealed two LGMNs which are 1,438 bp for isoform-1 (Figure 10) and 1,365 bp for isoform-2 (Figure 11) with 1,275 bp open reading frames of equivalent length. The ATG start codon was predicted at the nucleotides 26 to 28 for isoform-1 and 10 to 12 for isoform-2. Isoform-1 and -2 contain TGA stop codons at nucleotides 1,301 to 1,303 and 1,285 to 1,287, respectively. The polyadenylation signal sequence of isoform-1 was predicted at the nucleotides 1,390 to 1,395 with sequence of AATAAA and of isoform-2 at the nucleotides 1,304 to 1,308 with sequence of AATAA. These genes encode predicted proteins of 425 amino acid residues. The properties of nucleic acid sequences are summarized in Table 6.

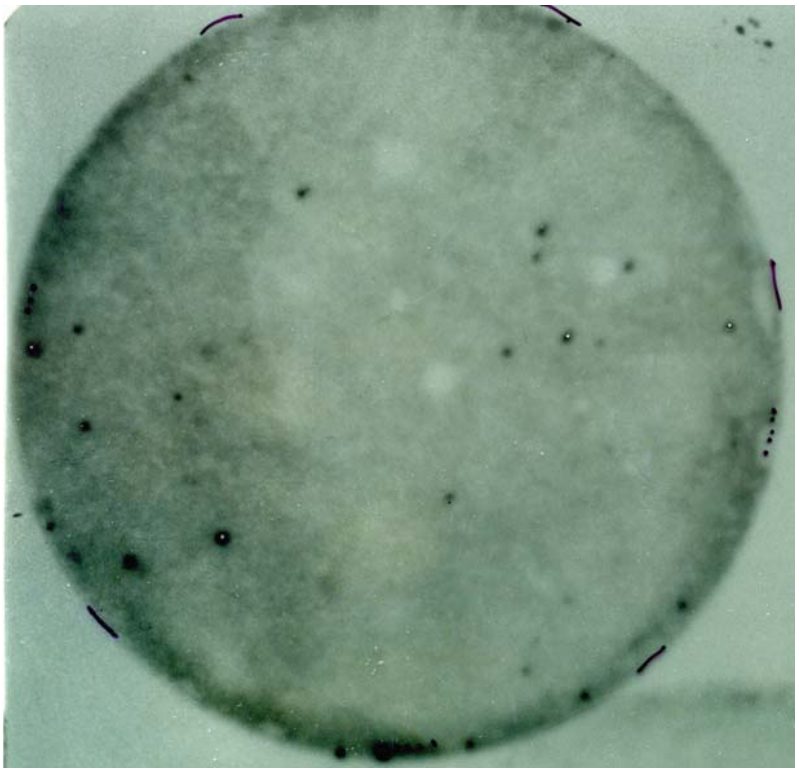

Figure 8 Screening of an adult stage *F. gigantica* cDNA library with a radioactive-^{32}P labeled legumain conserved probe. In high density screening, several positive clones were detected (black spots) and then picked to perform low density screening to obtain well-isolated full-length genes.

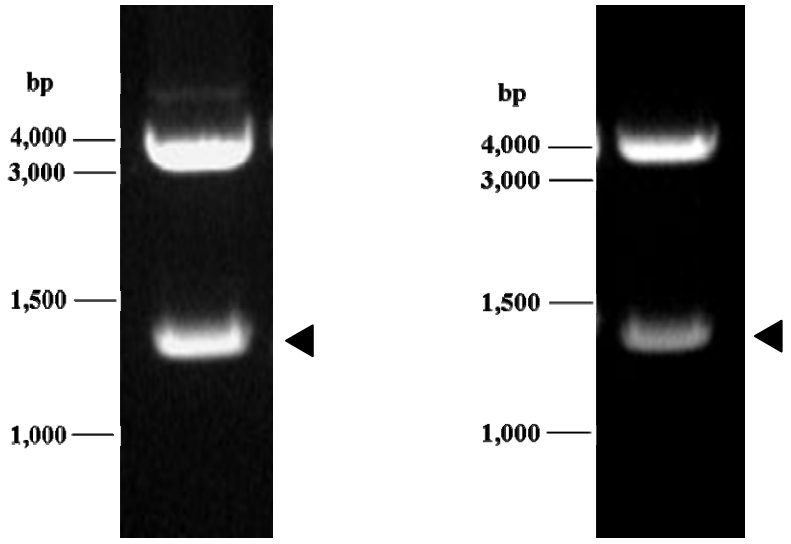

Figure 9 The recombinant pTriplEx2 phagemid containing full-length cDNAs of *F. gigantica* legumains were digested with *Kpn* I and *Xho* I restriction endonucleases. (A) FgLGMN-1. (B) FgLGMN-2 (Arrowheads).

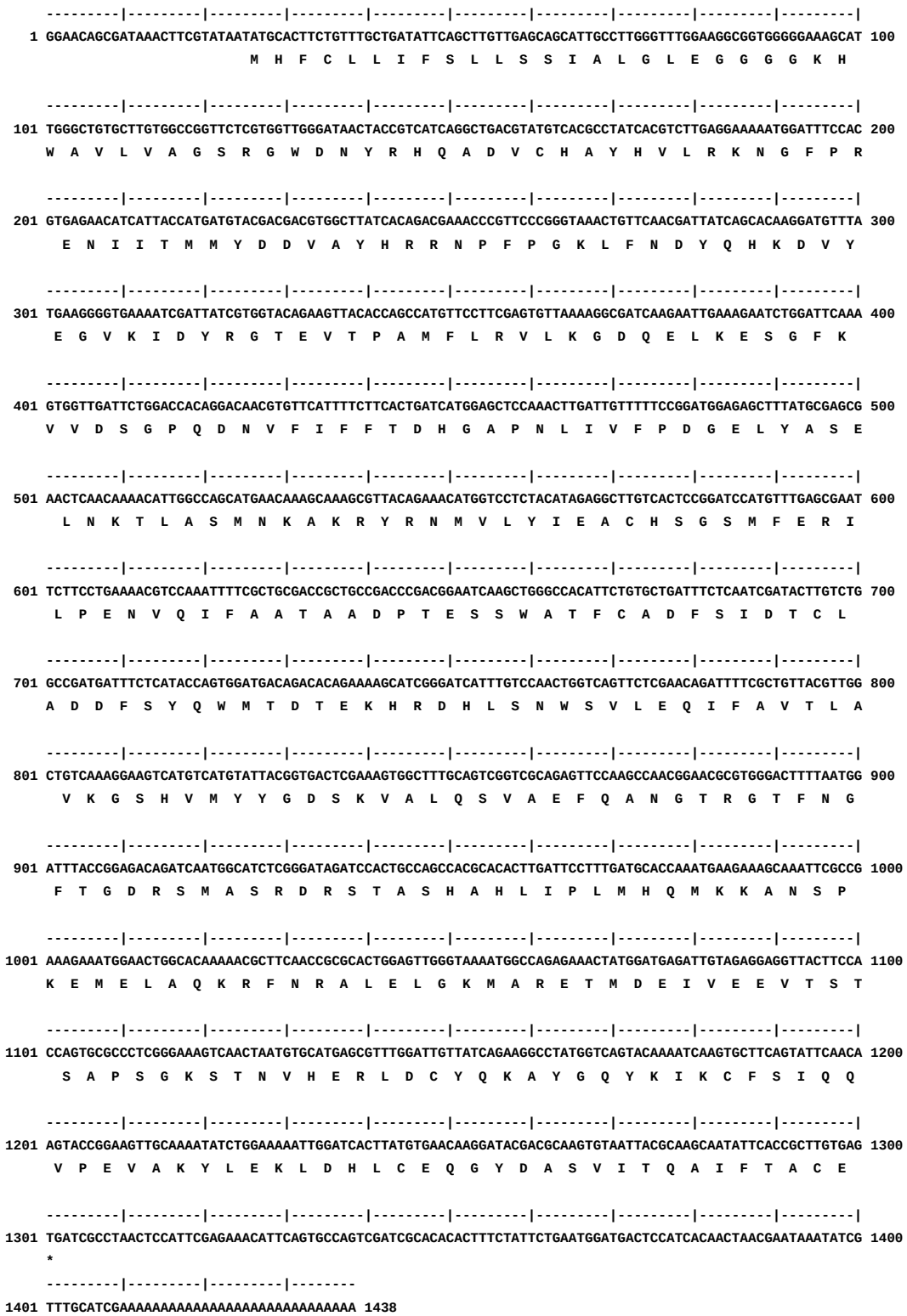

Figure 10 Full length nucleotide sequence with deduced amino acid sequence of legumain-1 FgLGMN-1 from *F. gigantica* (GenBank accession no. EF206821).

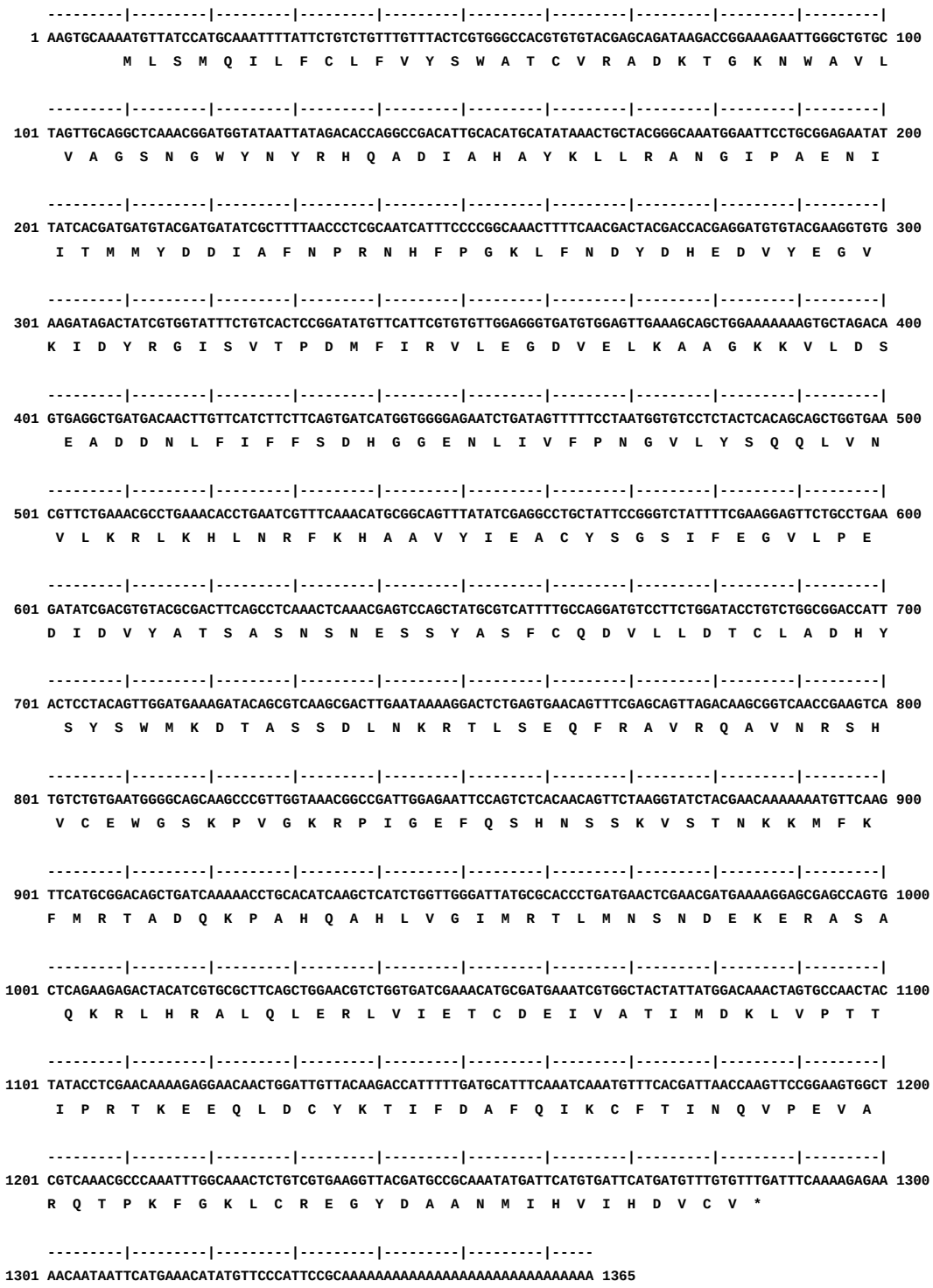

Figure 11 Full length nucleotide sequence with deduced amino acid sequence of legumain-2 FgLGMN-2 from *F. gigantica* (GenBank accession no. EF206822).

Table 6 Analysis of FgLGMN-1 and FgLGMN-2 nucleic acids

Properties	**FgLGMN-1**	**FgLGMN-2**
Full length (nt)	1,438	1,365
Open reading frame (nt)	1,275	1,275
Start codon	ATG (26-28)	ATG (10-12)
Stop codon	TGA (1,301-1,303)	TGA (1,285-1,287)
Polyadenylation signal	AATAAA (1,390-1,395)	AATAA (1,304-1,308)
Deduced amino acid (aa)	425	425

A homology search with GenBank database by NCBI-BLASTp showed that both deduced protein sequences belong to the legumain family of C13 family peptidases. The two novels LGMNs from *F. gigantica* are designated *F. gigantica* legumain 1 (FgLGMN-1) and legumain 2 (FgLGMN-2). The selected sequences that show high identity in each group of orthologs are given in Table 7. Particularly, FgLGMN-1 and -2 are 50% and 42% identical to *F. hepatica* LGMN (FhLGMN) (EMBL accession no. AJ250582). According to ortholog homology, they showed high score identity to closely related trematodes in the genera *Opisthorchis* and *Schistosoma*. The percentage identity with *Opisthorchis viverrini* (GenBank accession no. DQ402101) were 46% in equal value of both FgLGMN-1 and -2 and with *Schistosoma mansoni* (EMBL accession no. AJ250582) were 48% and 43%, respectively. The pairwise comparison of FgLGMN-1 and FgLGMN-2 showed 47% identity (Table 8). The isolated genes were submitted to the GenBank™ under the accession number EF206821 for FgLGMN-1 and EF206822 for FgLGMN-2.

Table 7 Selection of database matches of orthologs from the legumain (C13) family used in multiple alignments and phylogenetic tree analysis with FgLGMN-1 and FgLGMN-2.

Organism	**Homologs**	**Accession**
Fasciola gigantica	Legumain-1	GB/EF206821
Fasciola gigantica	Legumain-2	GB/EF206822
Fasciola hepatica	Legumain-like precursor	EMB/AJ314846
Opisthorchis viverrini	Legumain	GB/DQ402101
Schistosoma mansoni	Asparaginyl endopeptidase	EMB/AJ250582
Mus musculus (mouse)	Legumain	REF/NM_011175
Homo sapiens (human)	Legumain, preproprotein	GB/BC003061
Bos Taurus (cow)	Legumain	REF/NM_174101
Arabidopsis thaliana	Cysteine-type endopeptidase (DELTA-VPE)	REF/NM_112912
Vigna mungo	Asparaginyl endopeptidase (VmPE-1A)	DBJ/D89972
Trichomonas vaginalis	Legumain-like cysteine proteinase 1	GB/AY326447
Trichomonas vaginalis	Legumain-like cysteine proteinase 2	GB/AY326446

Table 8 Sequence identity/similarity matrix of orthologous legumain amino acid sequences

	FgLGMN-1	FgLGMN-2	FhLGMN	OvLGMN	SmLGMN	HsLGMN	VmPE-1A
FgLGMN-1	1	*0.64*	*0.68*	*0.65*	*0.62*	*0.55*	*0.52*
FgLGMN-2	**0.47**	1	*0.60*	*0.63*	*0.62*	*0.56*	*0.49*
FhLGMN	**0.50**	**0.42**	1	*0.59*	*0.56*	*0.50*	*0.45*
OvLGMN	**0.46**	**0.45**	**0.39**	1	*0.57*	*0.54*	*0.45*
SmLGMN	**0.48**	**0.43**	**0.39**	**0.42**	1	*0.54*	*0.50*
HsLGMN	**0.36**	**0.38**	**0.32**	**0.39**	**0.39**	1	*0.49*
VmPE-1A	**0.33**	**0.33**	**0.28**	**0.32**	**0.35**	**0.34**	1

The values of identity and similarity to FgLGMN-1 and FgLGMN-2 were calculated by NCBI-BLASTp. The value between orthologs were calculated by global pairwise alignments (EMBOSS needle, BLOSUM62 matrix with Gap_penulty: 10 and Extend_penulty: 0.5) of the full-length deduced amino acid sequences. Value in bold lettering indicate identity, value in italic lettering indicate similarity. The value 1 is equal to 100%.

1.4 Protein sequence characterization and phylogenetic relationships with ortholog LGMNs

The FgLGMN-1 cDNA encodes a predicted protease of 48.0 kDA with calculated p*I* of 6.5. The FgLGMN-2 cDNA encodes a predicted protease of 48.4 kDa with calculated p*I* of 7.2. Analysis of the N-terminus of the deduced amino acid sequences with the SignalP 3.0 World Wide Web Server (Bendtsen *et al*. 2004) indicated the presence of a signal peptide from residues 1-18 for FgLGMN-1 and 1-21 for FgLGMN-2. The predicted consensus sequences of a cleavage site at Leu^{18} and Glu^{19} for FgLGMN-1 and Ala^{21} and Asp^{22} for FgLGMN-2 are shown in Figure 12.

The prediction of N-glycosylation by NetNGlyc 1.0 Server (provided by Technical University of Denmark) showed three potential glycosylation sites in the deduced amino acid sequences of FgLGMN-1 and -2, at Asn^{161}, Asn^{246} and Asn^{284} for FgLGMN-1 (Figure 13A) and Asn^{210}, Asn^{261} and Asn^{285} for FgLGMN-2 (Figure 13B). The deduced amino acid properties are summarized in Figure 14.

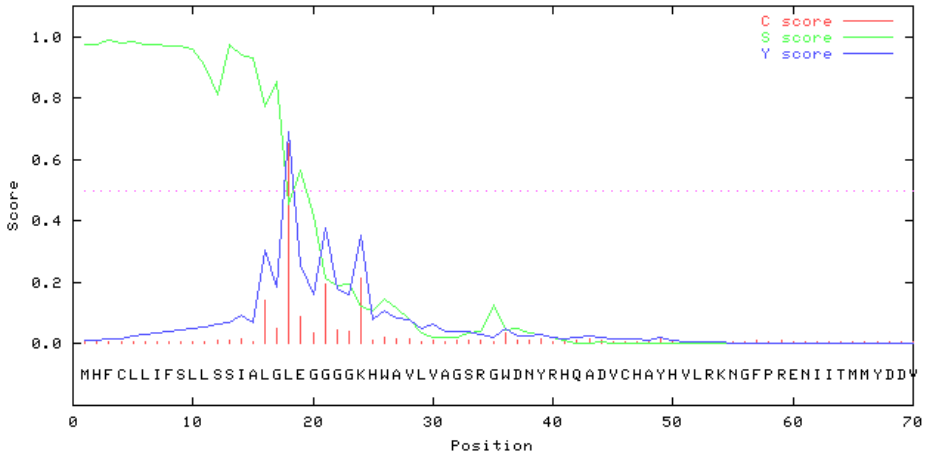

(A)

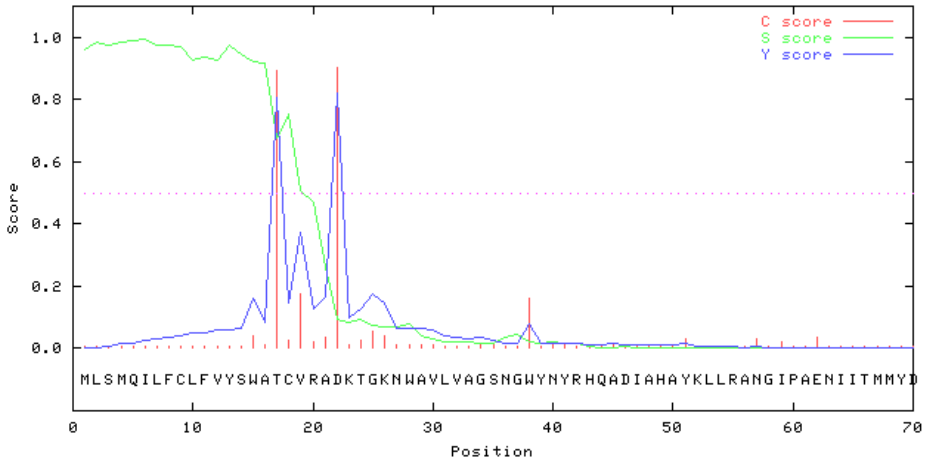

(B)

Figure 12 Predicted signal peptides of FgLGMNs. Figure A: FgLGMN-1, the putative signal peptide at the residues 1-18 by cleavage at Lysine 18 (K^{18}) and Glutamic acid 19 (E^{19}). Figure B: FgLGMN-2, the putative signal peptide at the residues 1-21 by cleavage at Alanine 21 (A^{21}) and Aspartic acid 22 (D^{22}).

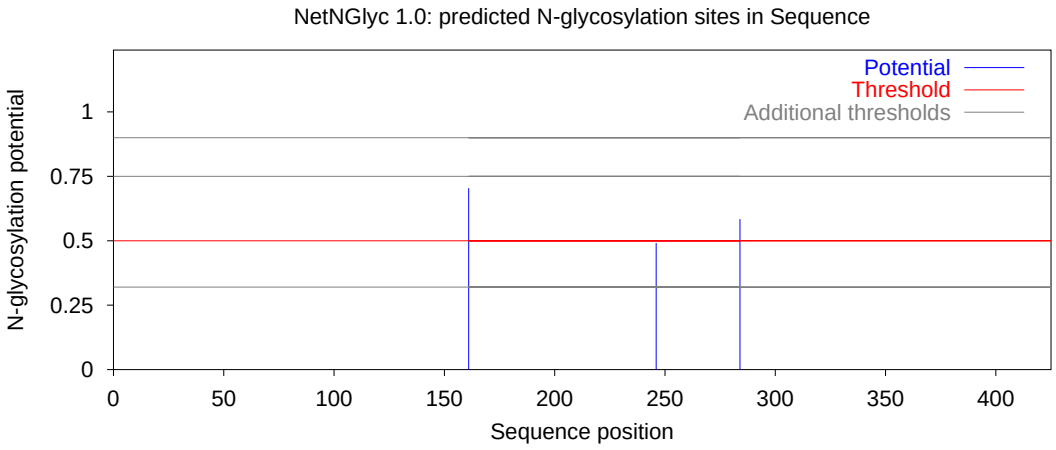

(A)

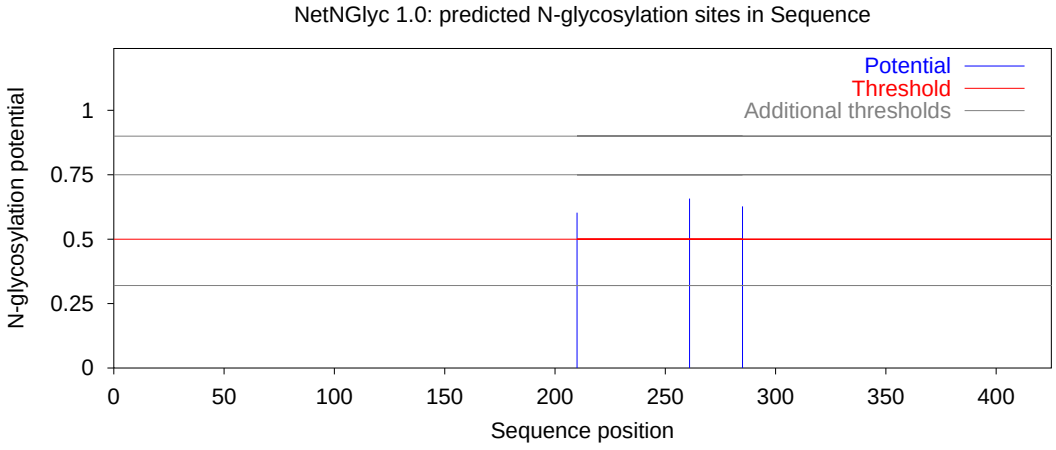

(B)

Figure 13 The prediction of N-glycosylation sites in FgLGMN-1 (Figure A) and FgLGMN-2 (Figure B). The blue bar indicates the potential glycosylation at Asparagine (N) residues; N^{161}, N^{246} and N^{284} for FgLGMN-1 and N^{210}, N^{261} and N^{285} for FgLGMN-2.

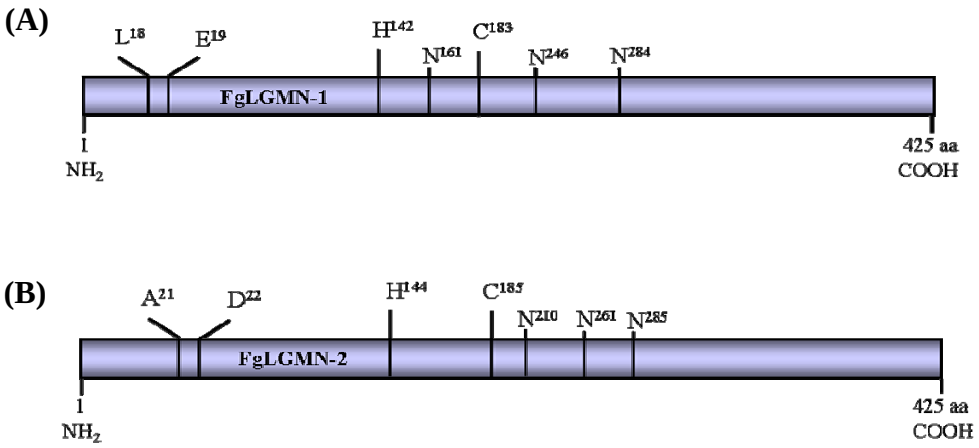

Figure 14 Diagrams of FgLGMN amino acid properties. The FgLGMN-1 (Figure A) and FgLGMN-2 (Figure B) proteins from *F. gigantica* that encoded by 425 amino acid residues. Diagrammatic representation of FgGMN-1 showing the putative signal peptide residues. The catalytic dyad histidine (H) and cysteine (C) residues and the predicted N-glycosylation sites.

Multiple alignment analysis of deduced amino acid sequences in selected ortholog amino acid sequences (Table 7) showed three highly conserved regions present in the legumain family. At the first conserved region, almost all orthologs contained the motif that is composed of Asn-Tyr-Arg-His-Glu-Ala Asp (NYRHQAD) (marked with * in Figure 15). The other two conserved regions located in the expected consensus regions of active site were observed at the catalytic dyad histidine and cysteine residues. The histidine is within the motif Xaa-Xaa-Xaa-Xaa-Xbb-Xbb-His-Gly-Xbb, in which Xaa is a hydrophobic amino acid and Xbb is a small amino acid (Ala, Asp, Glu, Gly, Ser or Thr) (marked with * in Figure 15). The cysteine is located in a motif, Xaa-Xaa-Xaa-Xaa-Xbb-Xbb-Cys (bold, marked with * in Figure 15).

In *F. gigantica* leumains, the catalytic dyad was found at the residues 142 and 183 for FgLGMN-1 and at residues 144 and 185 for FgLGMN-2 (bold, marked with #, Figure 8). In *F. hepatica*, cysteine in the catalytic dyad is replaced by serine (Cys191Ser, *F. hepatica* numbering). Similarly the inactive form of *S. mansoni* contains asparagines in place of cysteine (Cys197Asn, *S. mansoni* numbering). Additionally, six cysteine residues forming disulfide bridges were conserved in the legumain family. The conserved cysteine residues were found at the Cys^{216}, Cys^{224}, Cys^{375}, Cys^{387}, Cys^{407} and Cys^{424} for FgLGMN-1 and Cys^{218}, Cys^{226}, Cys^{375}, Cys^{387}, Cys^{407} and Cys^{424} for FgLGMN-2.

The conserved hydrophobicity pattern was observed in the active site of proteins of the legumain family (Figure 16). The conserve hydrophobic motifs have been seen in front of catalytic dyad (H and C) that was previously described. The conserve pattern was analyzed by CLUSTAL X as well and the color scheme showed the conserved residues around the catalytic dyad (Figure 17).

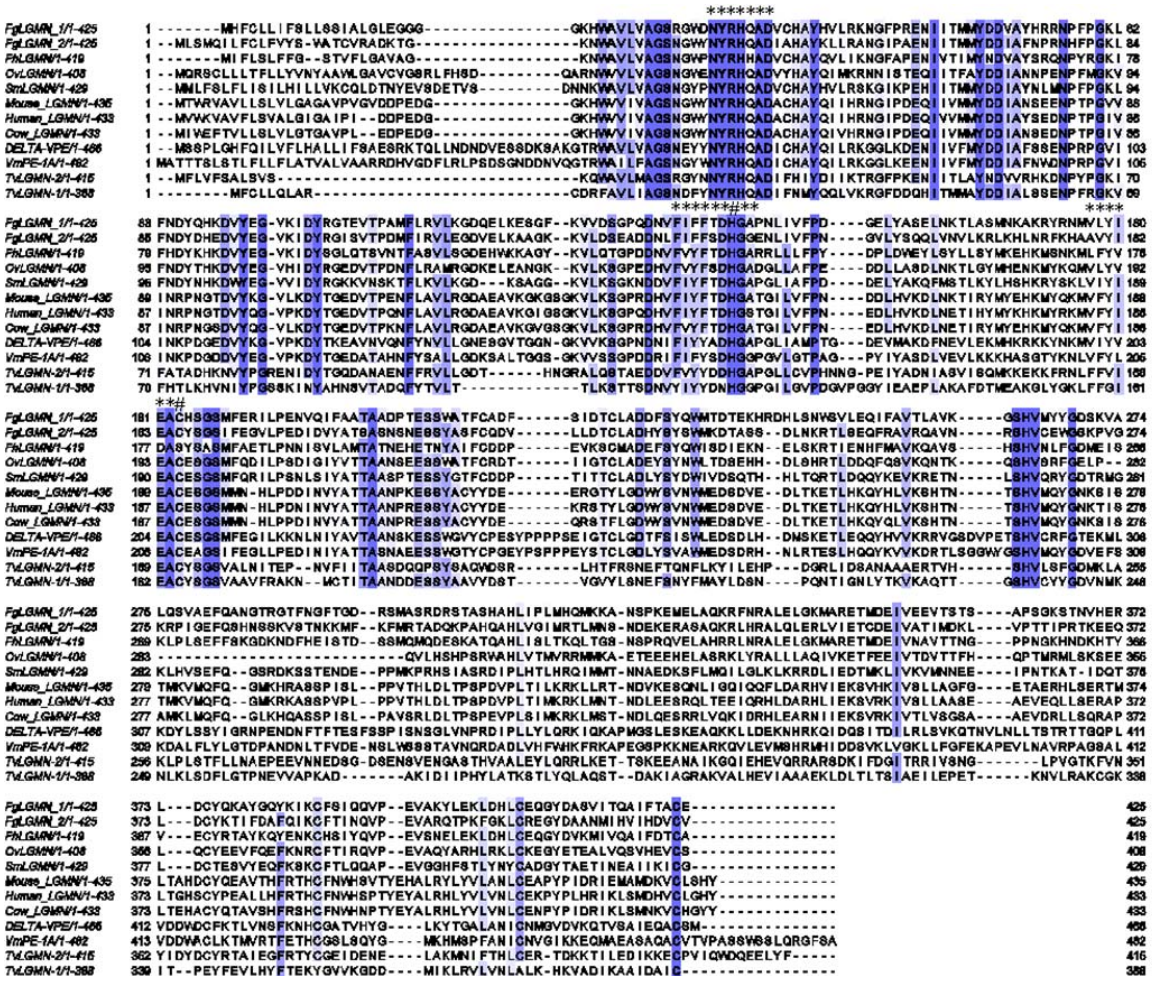

Figure 15 Multiple sequence alignment of legumains from plants (*A. thaliana* and *V. mungo*), protozoa (*T. vaginalis*), parasitic helminthes (*F. gigantica*, *F. hepatica*, *O. viverrini* and *S. mansoni*) and mammalians (human, mouse and cattle). The accession numbers of selected sequences are shown in table 2. The alignment was generated by Clustal W using the BLOSUM62 scoring matrix. A dash (-) indicates a missing residue, the asterisk (*) indicates a conserved residues and # indicates the catalytic dyad (H and C) residues. The color scheme was created by using percentage identity and background was reduced by using a criteria at 30% conservation; dark blue indicates >80% identity, blue indicates >60% identity, light blue indicates >40% identity and white indicates <40% identity. The graphic program was performed under JalView version 2.2 software (Clamp *et al*. 2004).

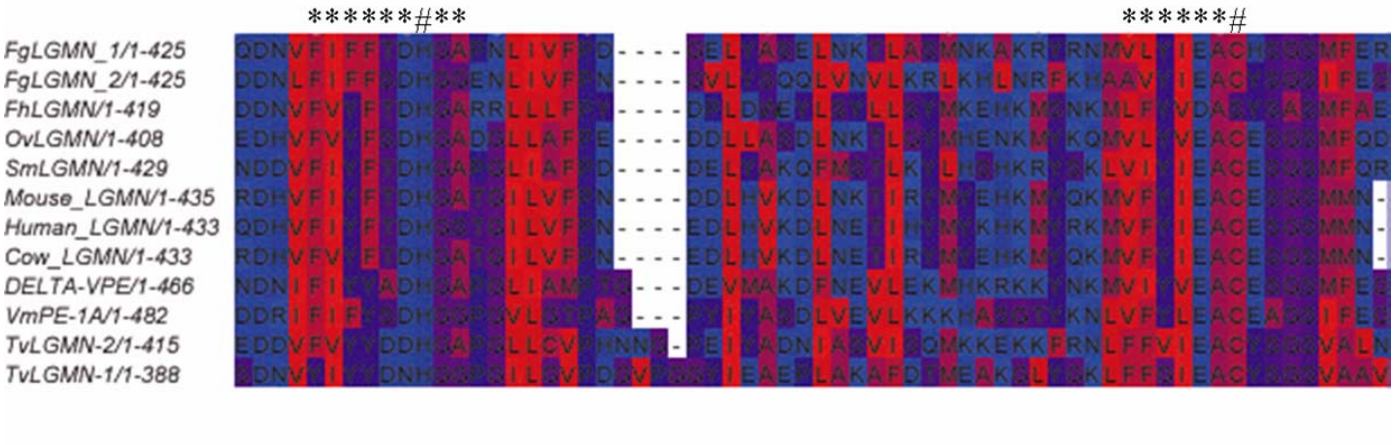

Figure 16 Multiple sequence alignment of legumains showing hydrophobic properties at the active site. The alignment was generated by Clustal W using the BLOSUM62 scoring matrix. A dash (-) indicates a missing residue, the asterisk (*) indicates a conserved residue and # indicates the catalytic dyad (H and C) residues; red indicates hydrophobic residues, blue indicates hydrophilic residues.

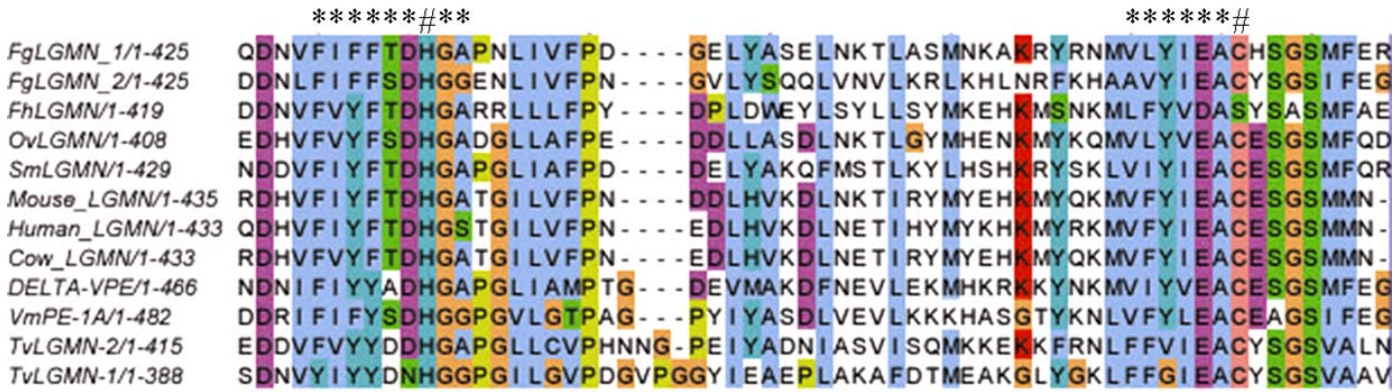

Figure 17 Multiple sequence alignment of legumains shown by CLUSTAL X at the active site. The alignment was generated by Clustal W using the BLOSUM62 scoring matrix. A dash (-) indicates a missing residue, the asterisk (*) indicates a conserved residues and # indicates the catalytic dyad (H and C) residues. The color scheme was created by using CLUSTAL X, Blue: A, I, L, M, F, W, V; red: R, K; green: N, Q, S, T; pink: C; margenta: E, D; orange: G; cyan: H, Y; yellow: P. The graphic program was performed under JalView version 2.2 software (Clamp *et al*. 2004).

The phylogenetic analysis was reconstructed by bootstrap-neighbor joining tree program based on Clustal W multiple sequence alignment (Saitou and Nei, 1987) (Figure 18). The bootstrap value is equal to 100. The entire deduced amino acid sequences of two FgLGMNs showed the closest relationship to LGMN of *F. hepatica* (EMBL accession no.AJ314846) belonging in the same genus. The close relationship has been seen in LGMNs of *S. mansoni* (EMBL accession no. AJ250582) as well as in *O. viverrini* (GenBank accession no. DQ402101). The legumains of trematode parasites were categorized in the same clade that were differentiated from mammalian legumains clade (human, mouse and cow) and plant legumain clade (Delta-VPE and VmPE-1A). The legumains of a protist, *T. vaginalis*, were categorized in outgroup that were previously proposed to be a new subgroup of legumain (León-Félix *et al*., 2004).

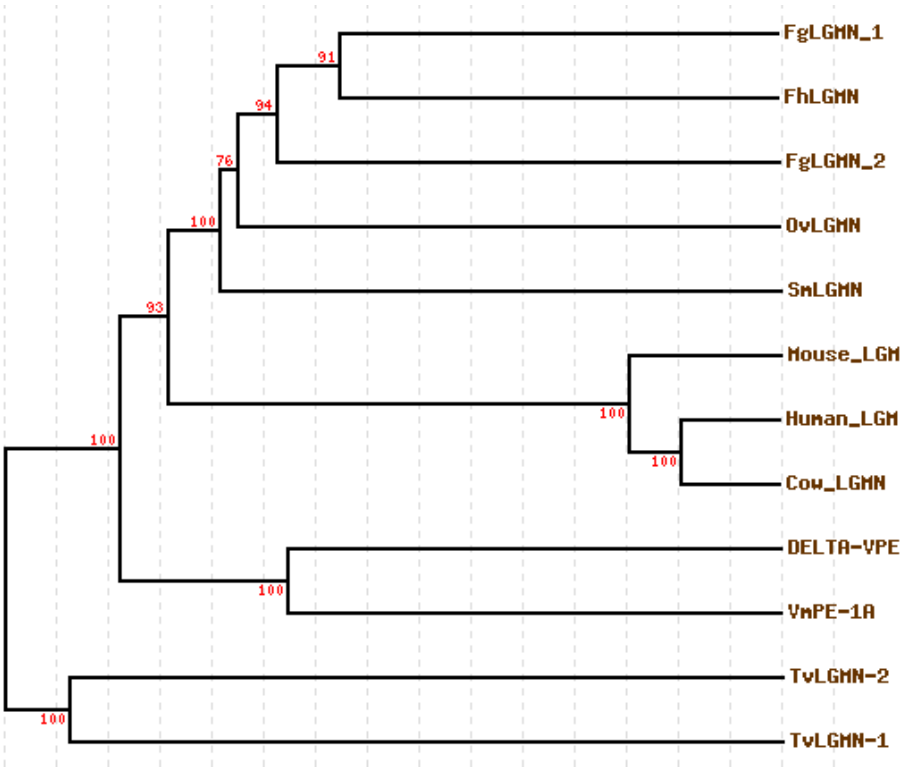

Figure 18 Phylogenetic tree of legumains. The selected amino acid sequences were obtained from GenBank using the accession numbers as described in Table 2. The phylogenetic tree was constructed by using bootstrap-neighbour joining tree method. The bootstrap value is equal to 100. Abbreviation see Figure 15.

2. Characterization of FgLGMN-1 and FgLGMN-2 genes in various developmental stages with respect to the isotypes and the gene expression

2.1 Southern hybridization analysis of *F. gigantica* genomic DNA with DIG-labeled LGMN-1 and LGMN-2 probes

FgLGMN-1 and -2 genes and their transcripts were performed under standard stringent hybridization conditions and the specific probe corresponding to DNA sequences does not cross-hybridize (Figure 19A and B). For Southern analysis, adult stage *F. gigantica* genomic DNA was digested with restriction endonucleases *Pae* I (*Sph* I) and *Pst* I. Both FgLGMN cDNAs do not contain recognition sites for these enzymes. The restricted genomic DNA fragments were hybridized with probes containing homologous putative mature FgLGMN encoding sequences. The FgLGMN-1 probe hybridized to six *Sph* I DNA fragments with sizes ranging from 1,500 to >21,000 bp, six *Sph* I/*Pst* I DNA fragments with size ranging from 1,500 to 21,000 bp, and three *Pst* I DNA fragments with sizes 3,600, 20,000 and >21,000 bp (Figure 20A). The FgLGMN-2 probe hybridized to two DNA fragments when cut by *Sph* I DNA fragments with sizes of 7,000 and 10,000 bp, five *Sph* I/*Pst* I DNA fragments with size ranging from 1,900 to 21,000 bp, and four *Pst* I DNA fragments with size ranging from 1,900 to 21,000 bp (Figure 20B).

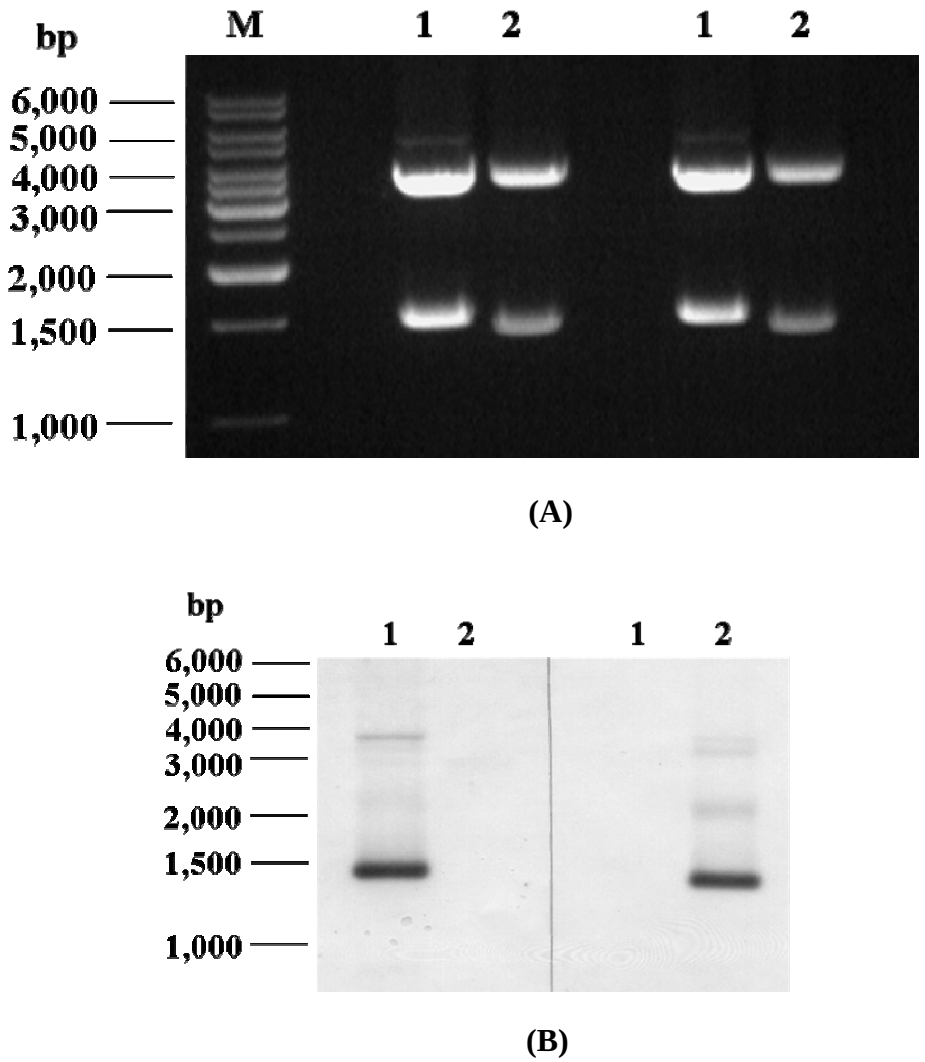

Figure 19 Cross-hybridization of *F. gigantica* legumain isoform-1 and isoform-2. Recombinant pTriplEx 2 vectors containing FgLGMN-1 (lane 1) and FgLGMN-2 (lane 2) were digested with *Kpn* I and *Xho* I (Figure A). After Southern hybridization, no cross-hybridization of the nucleic acids of the two isoforms was detected (Figure B); left panel: hybridization with FgLGMN-1 PCR probe, right panel: hybridization with FgLGMN-2 PCR probe. The correct size is determined with a 1 Kb DNA marker (lane M, Figure A) (Fermentas Life Sciences, Vilnius, Lithuania).

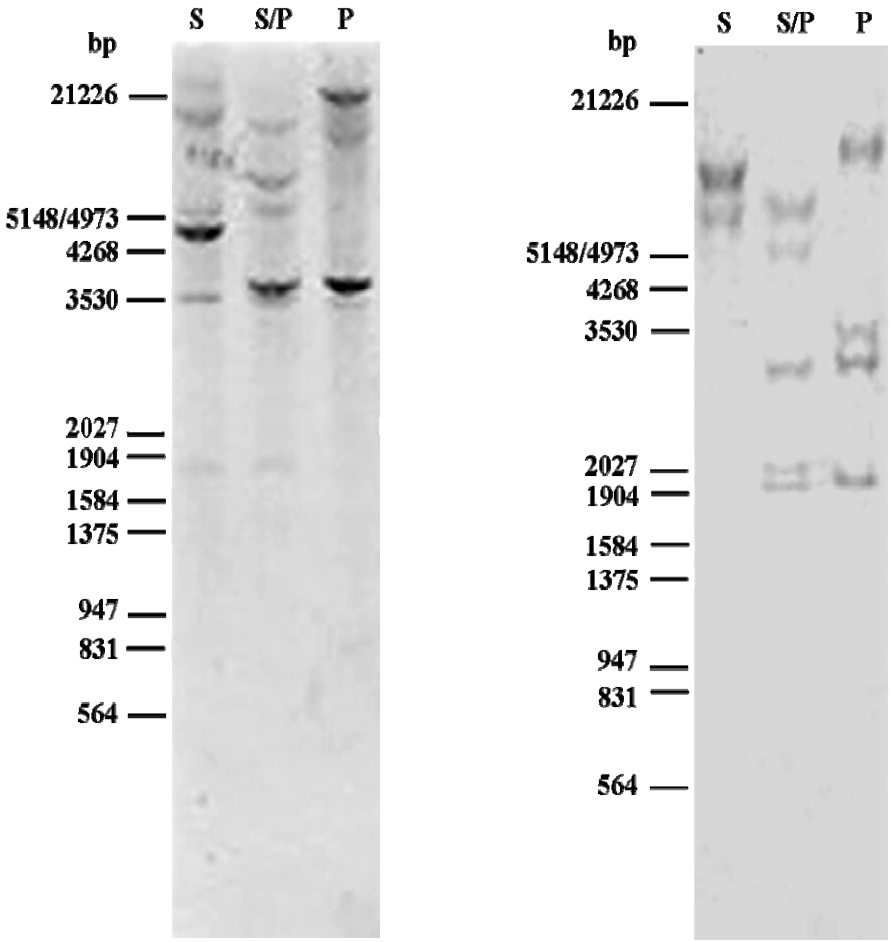

Figure 20 Southern hybridization of *F. gigantica* genomic DNA with DIG-labeled LGMN DNA probes; S: *Sph* I, S/P: *Sph* I/*Pst* I, or P: *Pst* I digested genomic DNA. Figure A, FgLGMN-1 hybridization DNA probe; Figure B, FgLGMN-2 hybridization DNA probe. The positions of the λ phage DNA cut with *Eco*R I and *Xho* I size standard fragments were indicated at the left side of each blot.

2.2 Gene transcription analysis by Northern hybridization and RT-PCR in different developmental stages of *F. gigantica*

2.2.1 Northern hybridization analysis

Total RNAs of 2-, 4- and 6-week old juveniles and adult *F. gigantica* were extracted and size-separated on a formaldehyde agarose gel and transferred to nylon membrane. The antisense specific FgLGMN-1 and -2 probes were used to detect specific mRNAs in total RNAs of different developmental stages of the parasites. All developmental stages total RNAs were hybridized with labeled anti-sense RNA probes of FgLGMN-1 at the molecular size of 2,400 nt (Figure 21) and FgLGMN-2 at the molecular size of 2,100 nt (Figure 22).

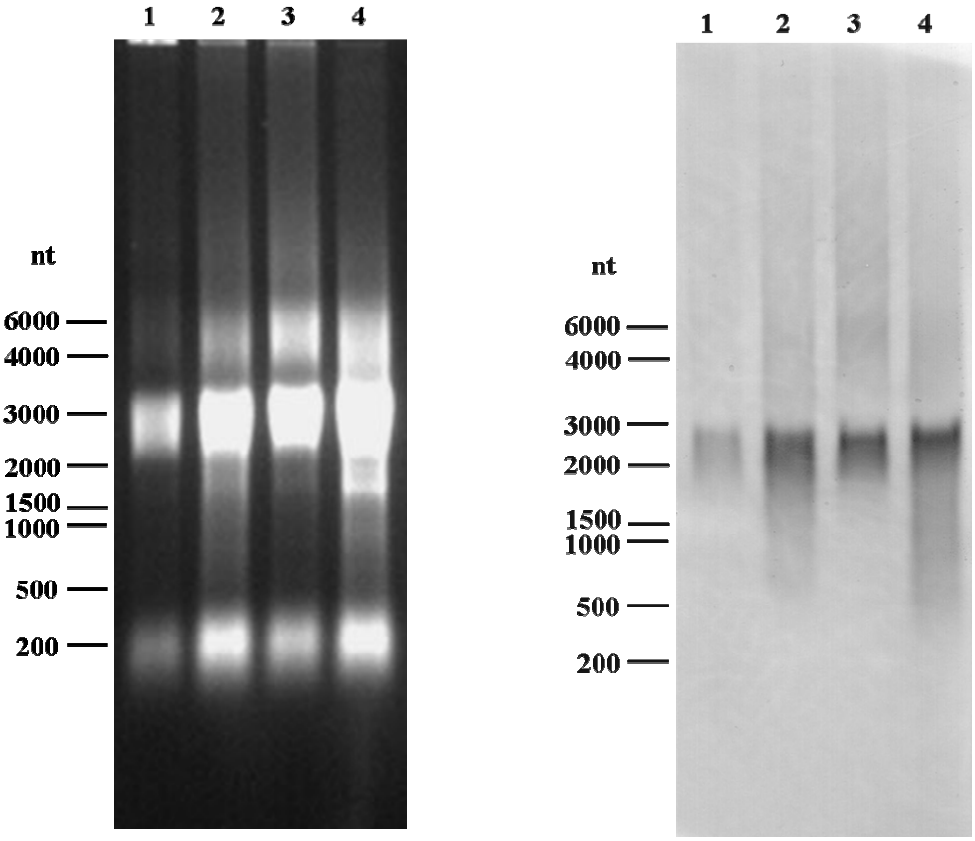

Figure 21 Northern hybridization of *F. gigantica* total RNA with FgLGMN-1 specific DIG-labeled RNA antisense probes; left: total RNA of 2-week (lane 1), 4-week (lane 2), 6-week (lane 3) old juveniles and adults (lane 4), size-separated by formaldehyde denaturing agarose gel elctrophoresis, right: after hybridization, DIG-labeled FgLGMN-1 antisense probe detected specific mRNA in all developmental stages. The positions of the RNA standard fragments are indicated at the left side.

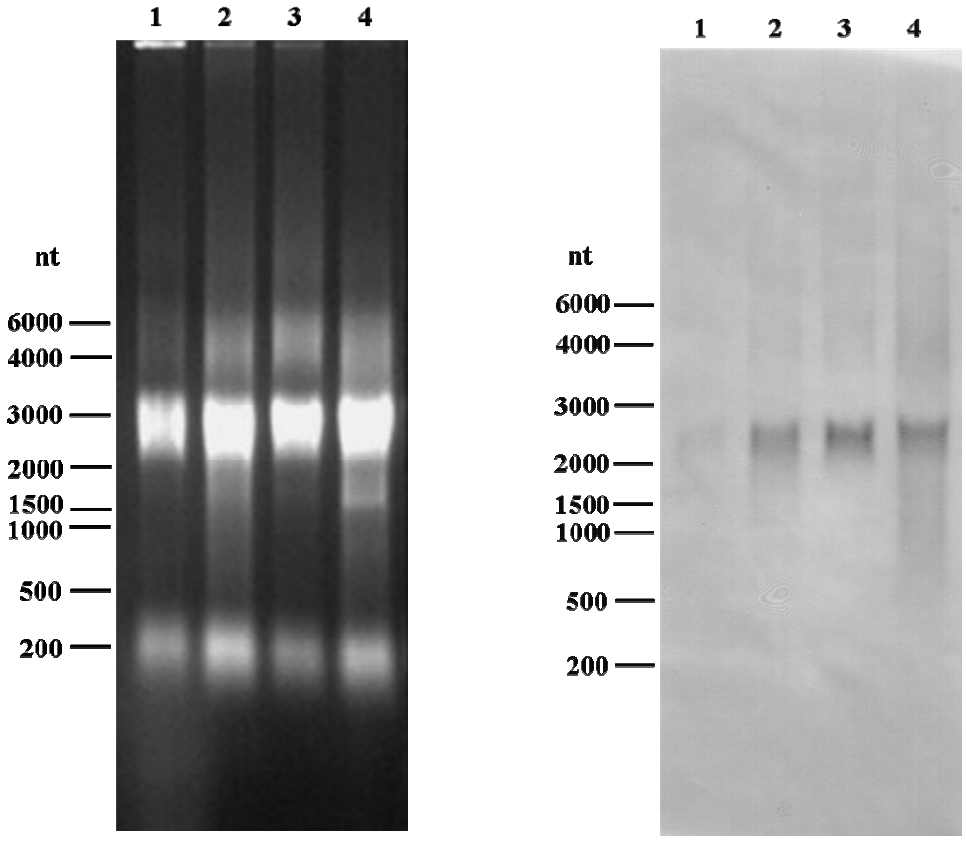

Figure 22 Northern hybridization of *F. gigantica* total RNA with FgLGMN-2 specific DIG-labeled RNA antisense probes; left: total RNAs of 2-week (lane 1), 4-week (lane 2), 6-week (lane 3) old juveniles and adults (lane 4), size-separated by formaldehyde denaturing agarose gel electrophoresis, right: after hybridization, DIG-labeled FgLGMN-1 antisense probe detected specific mRNA in all developmental stages. The positions of the RNA standard fragments are indicated at the left side.

2.2.2 Stage-specific RT-PCR

Total RNA of metacercariae, 1-, 2-, 4- and 6-week old juveniles and adult parasites was used to amplify specific cDNAs with specific primers designed for full open reading frames of the FgLGMN-1 and -2 genes. The RT-PCR products, analyzed in a native agarose gel, showed a specific product in a size of 1,275 bp and specificity was confirmed by Southern analysis. The RT-PCR products from different developmental stages were transferred onto a nylon membrane and hybridized with specific probes following Southern hybridization standard protocol. The RT-PCR products of FgLGMN-1 appeared at a size of 1,275 bp in 1-, 2-, 4- and 6-week juvenile and adult parasites but not in metacercariae. Consistently, The RT-PCR products on the nylon membrane were specifically hybridized with FgLGMN-1 probe (Figure 23A). For FgLGMN-2, The RT-PCR was performed with specific primers of FgLGMN-2. The FgLGMN-2 cDNAs were analyzed in a native agarose gel and showed the products of 1,275 bp in all developmental stages (metacercariae, 1-, 2-, 4- and 6-week juveniles and adult). Southern analysis confirmed the specificity with a FgLGMN-2 probe in all developmental stages (metacercariae, juveniles and adults) (Figure 23B).

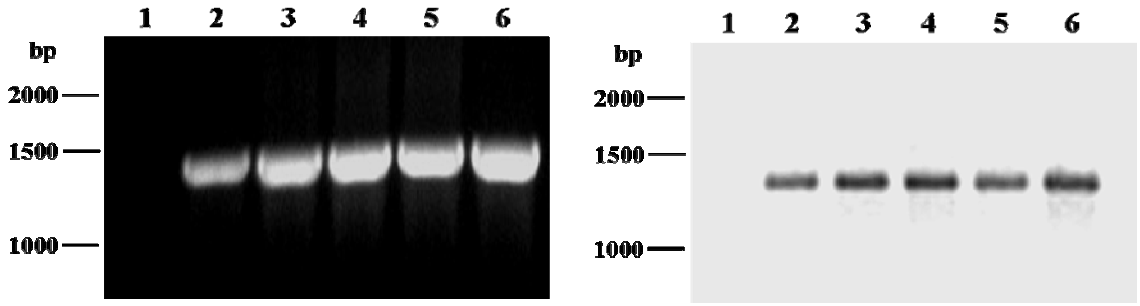

(A)

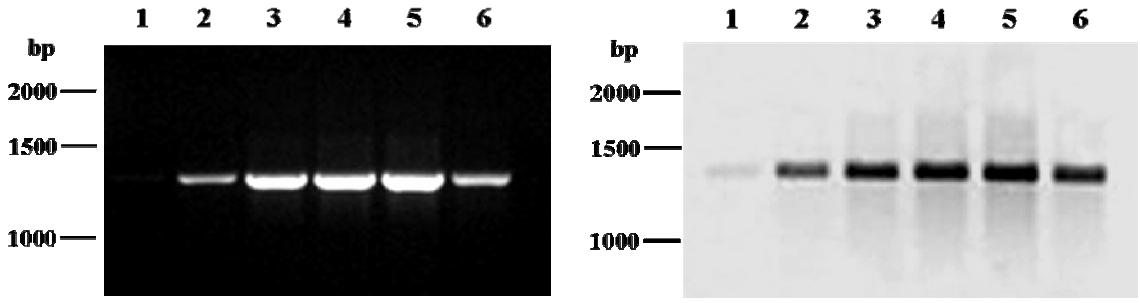

(B)

Figure 23 RT-PCR analysis of *F. gigantica* total RNA from metacercariae (lane 1), 1-week (lane 2), 2-week (lane 3), 4-week (lane 4), 6-week (lane 5) old juveniles and adults (lane 6) with gene-specific primers for FgLGMN-1 and FgLGMN-2, hybridized with DIG-labeled LGMN DNA probes; A: FgLGMN-1 PCR products (left) and hybridization with FgLGMN-1 DNA probe (right), B: FgLGMN-2 PCR products (left) and hybridization with FgLGMN-2 DNA probe (right). The positions of the 1 Kb DNA standard fragments are indicated at the left side.

3. Detection of FgLGMN-1 and FgLGMN-2 transcripts distributed in the tissues of *F. gigantica* in different developmental stages

The localization of legumains in *F. gigantica* tissues was detected by *in situ* hybridization. The tissue sections of 4-week old juveniles and adult parasites were hybridized with DIG-labeled anti-sense RNA transcribed from FgLGMN-1 and -2 cDNAs. The sections were also hybridized with the DIG-labeled sense RNA as the negative control. The FgLGMN-1 mRNA was specifically localized in gastrodermal epithelial cells in the digestive tract of adult parasites (Figures 24A, B, D and E). The FgLGMN-1 was localized in the cytoplasm of gastrodermal epithelial cells but not in the nuclei (hollow: arrow indicated, Figure 24E) corresponding to the location of mature mRNA. Other tissues; such as oral sucker, ventral sucker, cirrus tissue, eggs, tegument and reproductive organs (ovary, testis, prostate and uterus) of the adult parasite showed negative results for FgLGMN-1 mRNA localization (Figures 25A-E). The hybridization of tissue sections with the DIG-labeled FgLGMN-1 sense RNAs gave no signal in adult (Figure 24C) and 4-week old juvenile parasites (Figure 26C). In 4-week old juvenile parasite, the localization of FgLGMN-1 mRNA was consistent with adult stage parasites. The gut-specific localization is along the transverse full length section (Figure 26A) but not in other tissues. At high magnification, the positive signal confirmed the specific localization in the gastrodermal epithelial cells (Figure 26B).

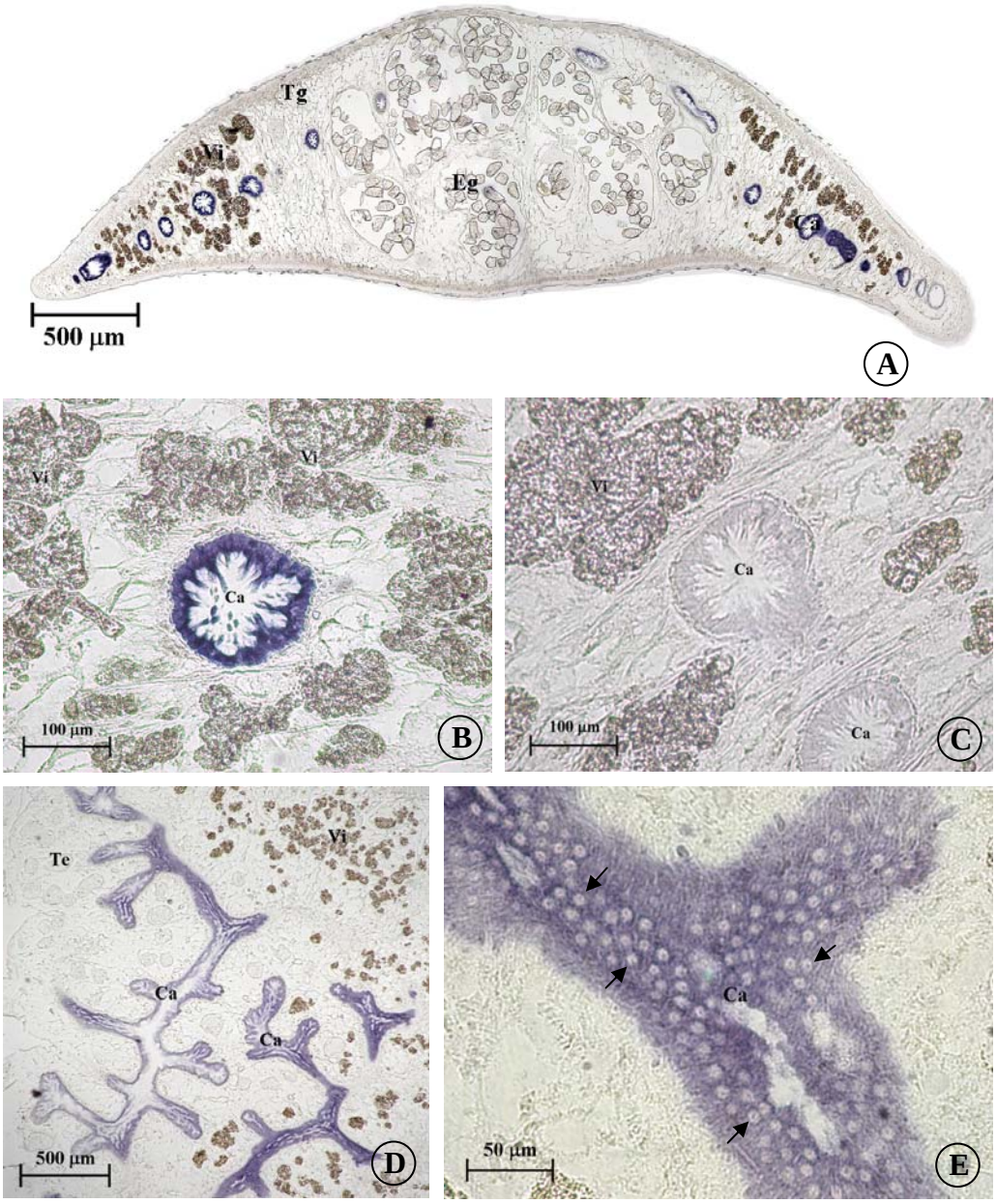

Figure 24 *In situ* hybridization of legumain-1 RNA in adult *F. gigantica* using FgLGMN-1 specific DIG-labeled RNA anti-sense probe. A: whole cross-section of an adult parasite, showing the localization of FgLGMN-1 mRNA restricted to the gastrodermal epithelium. B: higher magnification of a cross-section of an adult parasite. C: negative control hybridized with FgLGMN-1 sense probe. D: longitudinal section of an adult parasite. E: high magnification of longitudinal section of an adult parasite; the arrow indicates no staining in the nucleus. Ca: caecum; Eg: egg; Te: Testis; Tg: tegument; Vi: vitelline gland

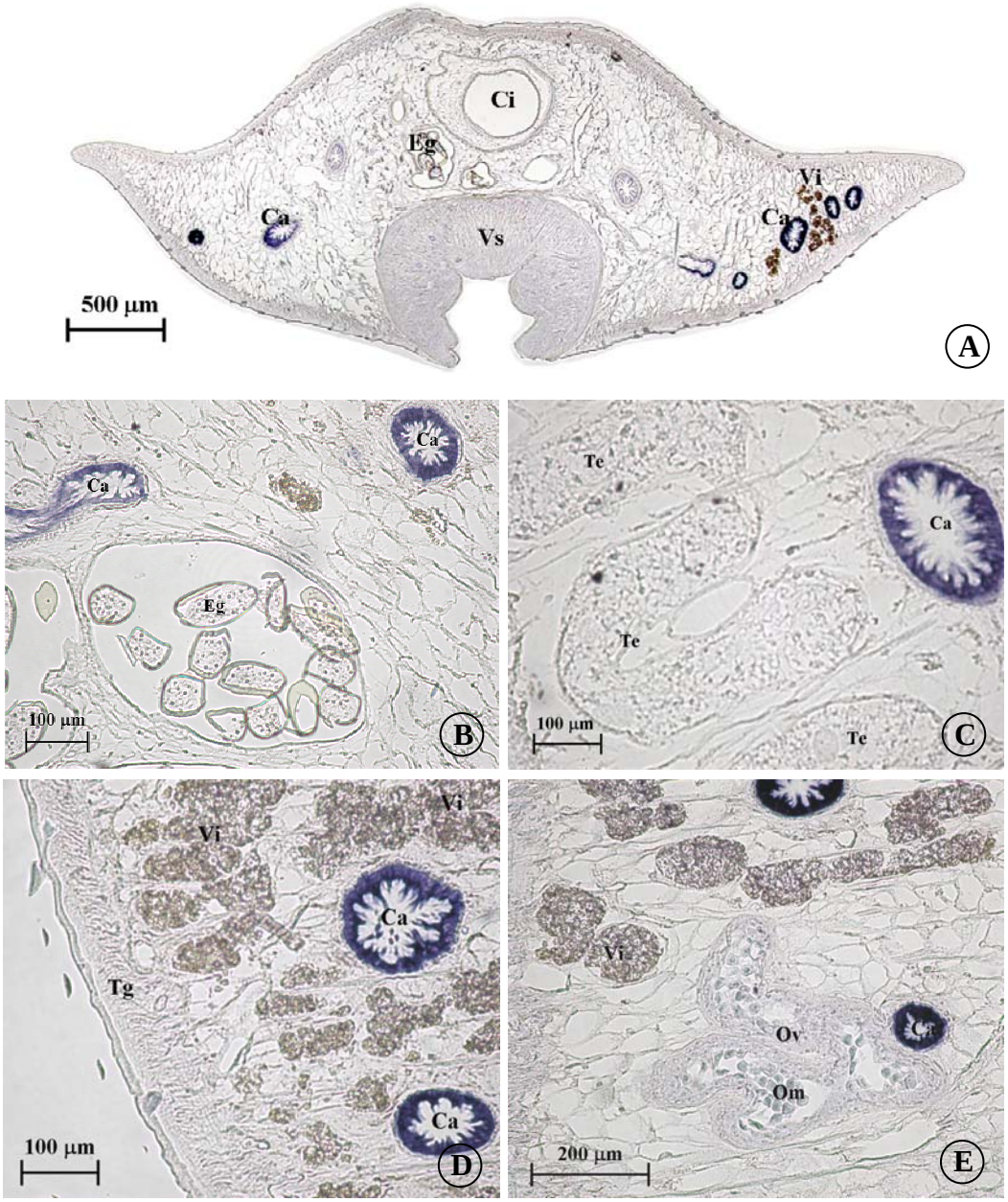

Figure 25 *In situ* hybridization of FgLGMN-1 RNA showed specific localization in the gastrodermal epithelial cells but not in other organs of the adult stage of *F. gigantica*. A: adult, whole cross-section of anterior part contained ventral sucker (Vs) and Cirrus tissue (Ci); B: negative staining of eggs (Eg) in the uterus compared to positive staining of gut; C: Testes (Te); D: Tegument (Tg); E: Ovary (Ov) containing Ovum (Om)

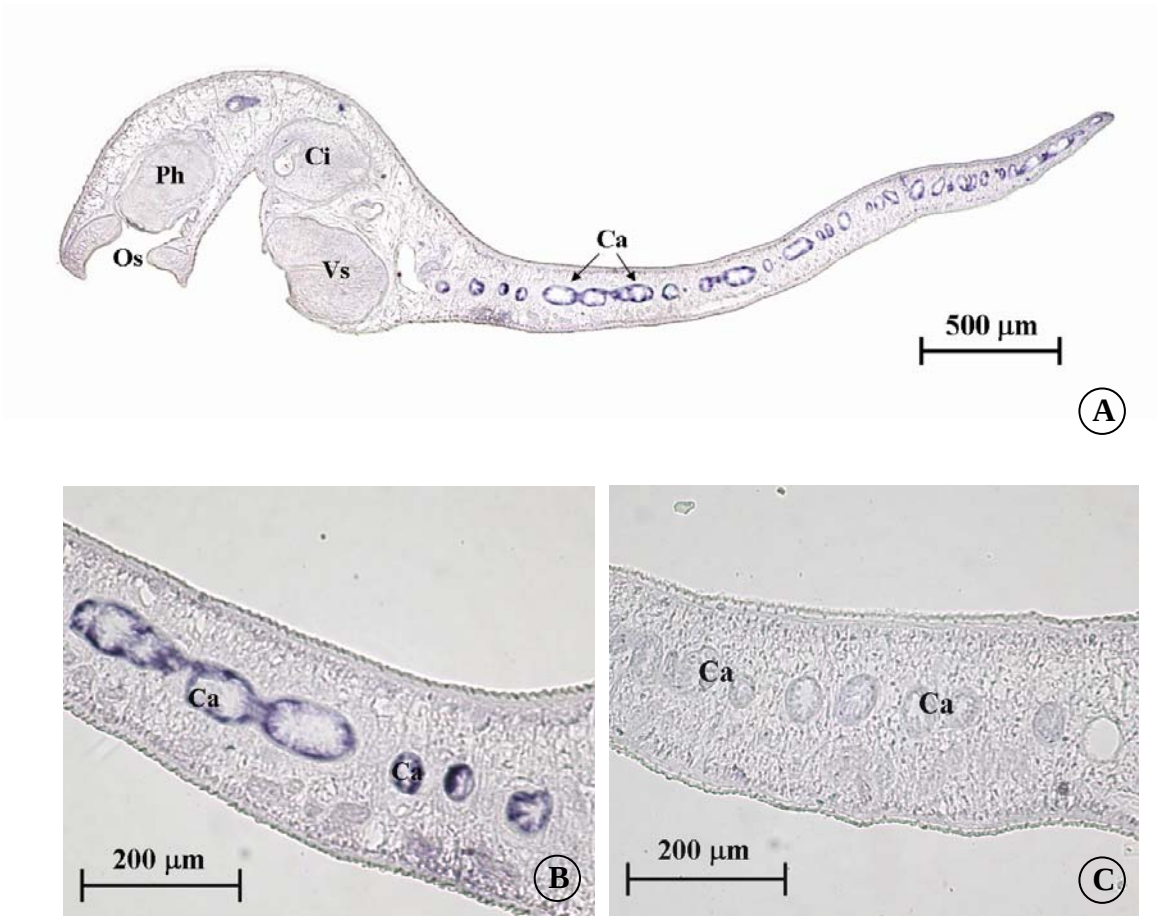

Figure 26 *In situ* hybridization of legumain-1 RNA in 4-week old juvenile *F. gigantica* using FgLGMN-1 specific DIG-labeled RNA anti-sense probe. A: full length sagittal section of a 4-week old juvenile showed specific localization of FgLGMN-1 mRNA at gastrodermal epithelial cells. B: higher magnification of a sagittal section of a 4-week juvenile parasite. C: negative control hybridized with FgLGMN-1 sense probe. Ca: caecum; Ci: cirrus porous; Os: oral sucker; Ph: pharynx and Vs: ventral sucker

The FgLGMN-2 mRNA was detected in the gastrodermal epithelial cells in digestive tract of adult (Figure 27) and juvenile *F. gigantica* (Figures 29 and 30) as same as FgLGMN-1 mRNA. In other tissues of the adult parasite, the FgLGMN-2 antisense probe could not detect the specific mRNA (Figures 28A-D). The longitudinal section of the anterior of the parasite showed negative staining in the upper digestive tract including mouth, pharynx and esophagus (Figure 28B). The localization of FgLGMN-2 mRNA at the caecal bifurcate suggests that the specific mRNA is transcribed in epithelial cells of specific tissue type specific in the caecum but not in the epithelial types in the upper digestive tracts (Figure 28C). In 4-week juveniles, FgLGMN-2 mRNA was localized in the gut epithelium as well (Figures 29A and B) but weak positive signal was detected though repeating and increasing the concentration of the probe. The concentration of the probe was varied from 10 to 100 ng. The localization of the FgLGMN-2 mRNA in juveniles was confirmed in 6-week old juvenile parasites that is clearly localized in gastrodermal epithelial tissues (Figure 30).

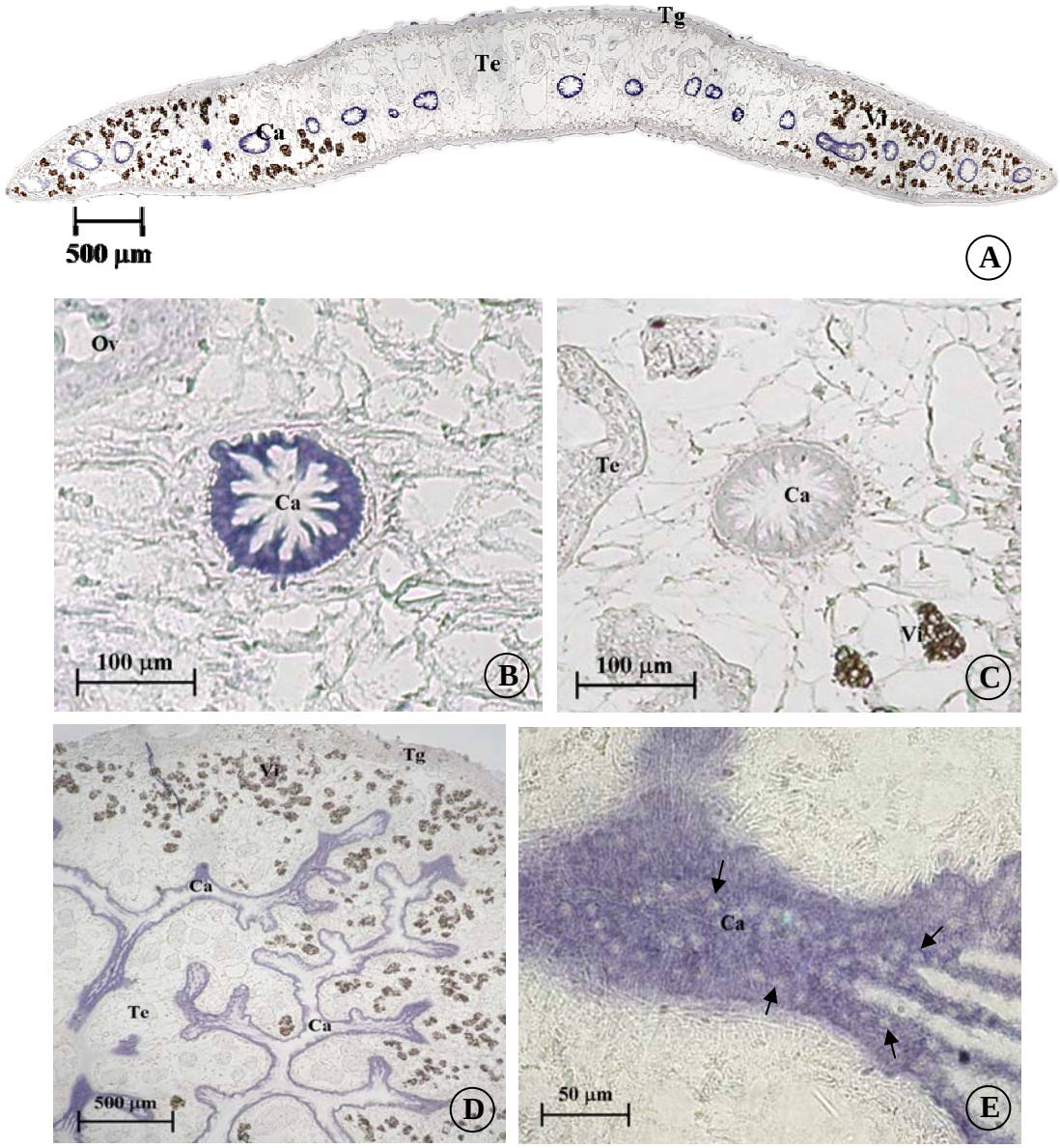

Figure 27 *In situ* hybridization of legumain-2 RNA in adult stages of *F. gigantica* using FgLGMN-2 specific DIG-labeled RNA anti-sense probe. A: whole cross-section of an adult parasite, showing the positive localization of FgLGMN-2 mRNA restricted to the gastrodermal epithelium. B: higher magnification of a cross-section of an adult parasite. C: negative control hybridized with FgLGMN-2 sense probe. D: longitudinal section of an adult parasite. E: high magnification of a longitudinal section of an adult parasite; arrow indicates no staining in the nucleus. Ca: caecum; Eg: egg; Ov: ovary; Te: Testis; Tg: tegument; Vi: vitelline gland

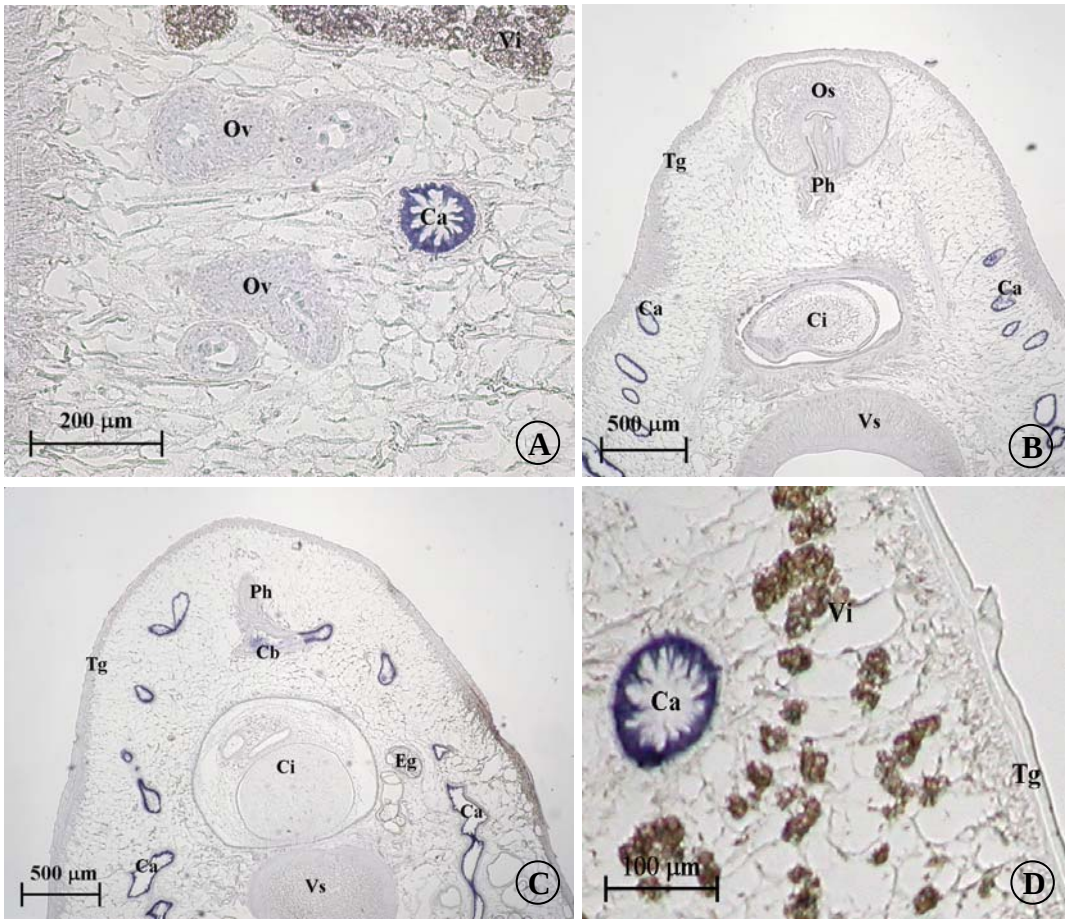

Figure 28 *In situ* hybridization of FgLGMN-2 RNA to different tissues of adult parasites. Gut-specific transcription was detected, because a clear signals appear in the gut epithelium but not in others. A: cross-section of ovary (Ov); B, C: longitudinal section of the adult parasite at the anterior part; D: the surface of the adult parasite. Ca: caecum; Cb: caecal bifurcate; Ci: Cirrus tissue; Eg: egg; Ph: pharynx; Os: oral sucker; Ov: ovary; Te: Testis; Tg: tegument; Vi: vitelline gland; Vs: ventral sucker

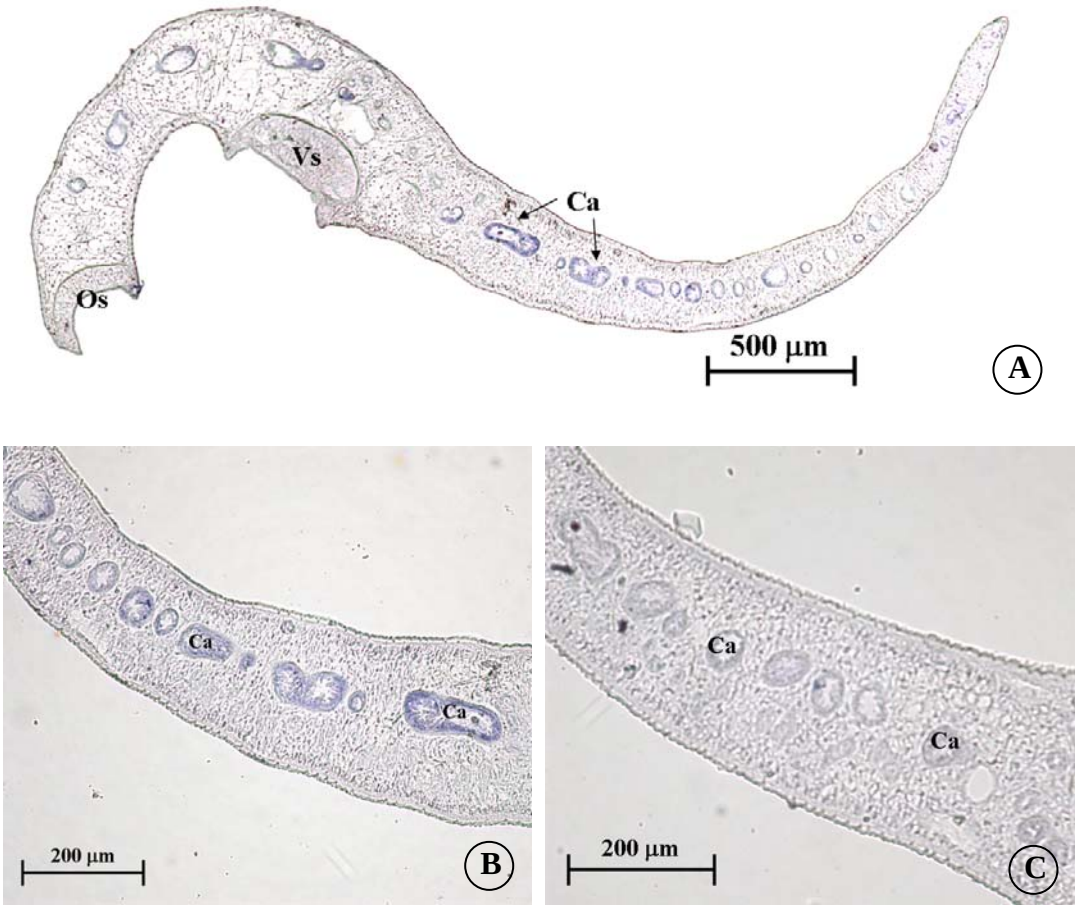

Figure 29 *In situ* hybridization of legumain-2 RNA to 4-week old juvenile *F. gigantica* using FgLGMN-2 specific DIG-labeled RNA anti-sense probe. A: full length sagittal section of a 4-week old juvenile showed specific localization of FgLGMN-2 mRNA at gastrodermal epithelial cell. B: higher magnification of sagital section of a 4-week juvenile parasite. C: negative control hybridized with FgLGMN-2 sense probe. Ca: caecum; Os: oral sucker; and Vs: ventral sucker

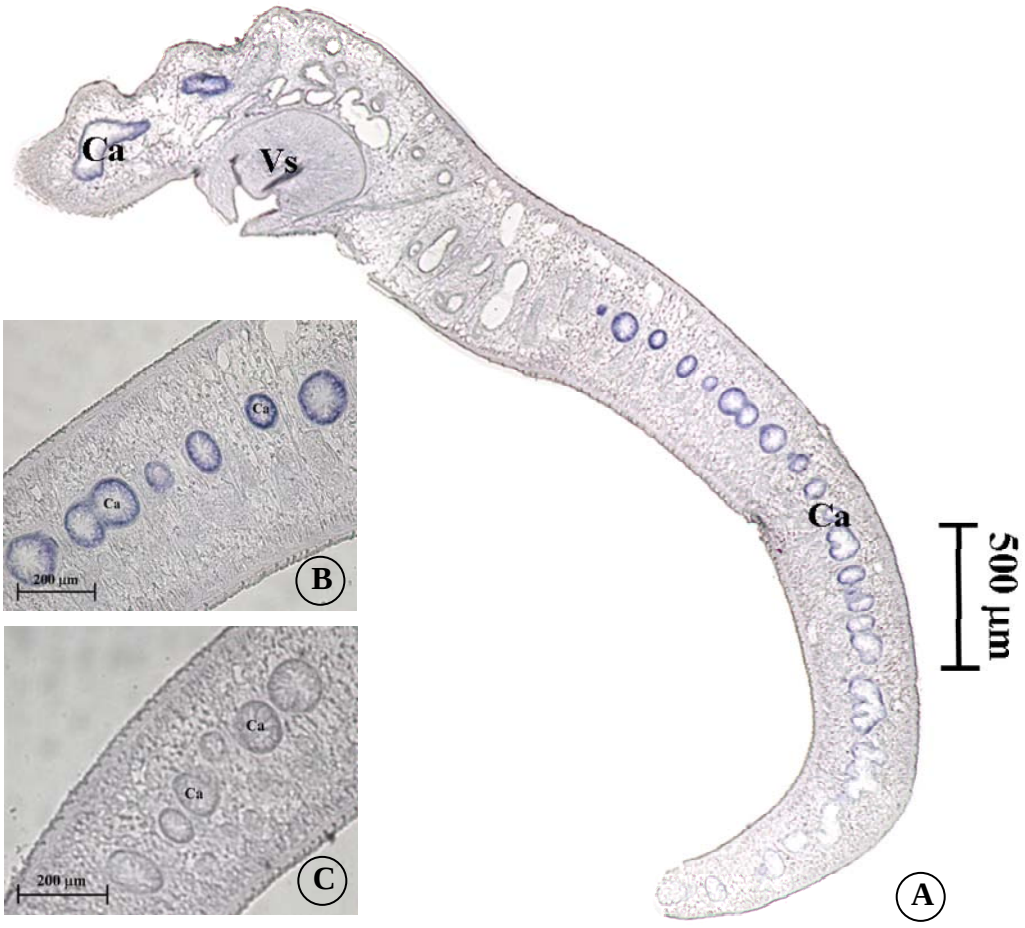

Figure 30 *In situ* hybridization of legumain-2 RNA to 6-week old juvenile *F. gigantica* using FgLGMN-2 specific DIG-labeled RNA anti-sense probe. A: full-length sagittal section of a 6-week old juvenile showed specific localization of FgLGMN-2 mRNA at gastrodermal epithelial cells. B: higher magnification of a sagittal section of a 6-week juvenile parasite. C: negative control hybridized with FgLGMN-2 sense probe. Ca: caecum and Vs: ventral sucker

4. Expression, purification of recombinant FgLGMN-1 and FgLGMN-2 proteins and antibody production

4.1 Subcloning of the FgLGMN cDNAs into the pET20b(+) prokaryotic expression vector

Partial FgLGMN cDNAs where the region encoding the signal peptide was deleted were unidirectional subcloned into the pET20b(+) prokaryotic expression vector between the *Hin*d III and *Xho* I recognition sites. *E. coli* BL21(DE3)pLysS were transformed with the recombinant plasmids. The transformants were verified by PCR and digestion of the obtained recombinant pET20b(+)/FgLGMN plasmid DNAs with *Hin*d III and *Xho* I. The PCR products were analyzed by 1% agarose gel electrophoresis that demonstrated clones size at approximately 1,200 bp (the calculated size of the fragment with the deleted signal peptide was 1,221 bp) for FgLGMN-1 cDNA (Figure 31A) and 1,200 bp (the calculated size of the fragment with the deleted signal peptide was 1,212 bp) for FgLGMN-2 cDNA (Figure 31B). In consistent with PCR, the cDNA fragment that were digested from the recombinant pET20b(+) plasmid showed the expected sizes for FgLGMN-1 (Figure 32, lane 1 and 2) and FgLGMN-2 (Figure 32, lane 3 and 4).

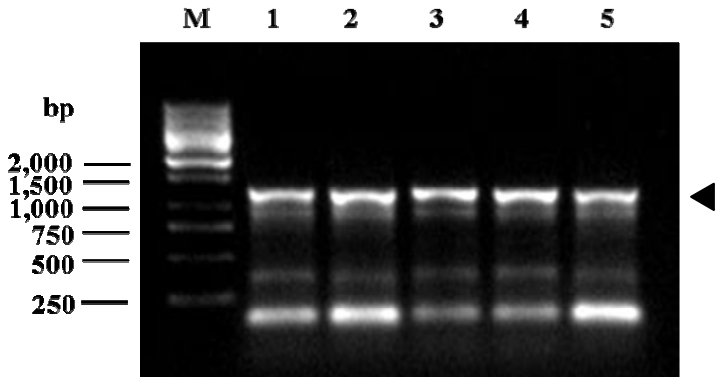

(A)

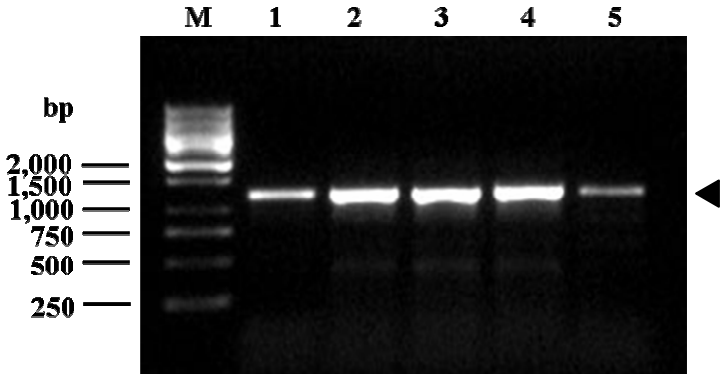

(B)

Figure 31 PCR amplification of FgLGMN-1 and -2 from colonies of transformed *E. coli* BL21(DE3)pLysS carrying recombinant pET20b(+). Figure A: five colonies of BL21(DE3)pLysS transformed with recombinant pET20b(+)/FgLGMN-1 were picked and amplified by PCR. Figure B: five colonies of BL21(DE3)pLysS transformed with recombinant pET20b(+)/FgLGMN-2 were picked and amplified by PCR. Arrow head indicates an expected fragment size and the positions of the 1 Kb DNA standard fragments are indicated at the left side. Lane M: 500 ng of 1 Kb DNA marker (Fermentas Life Sciences, Vilnius, Lithuania).

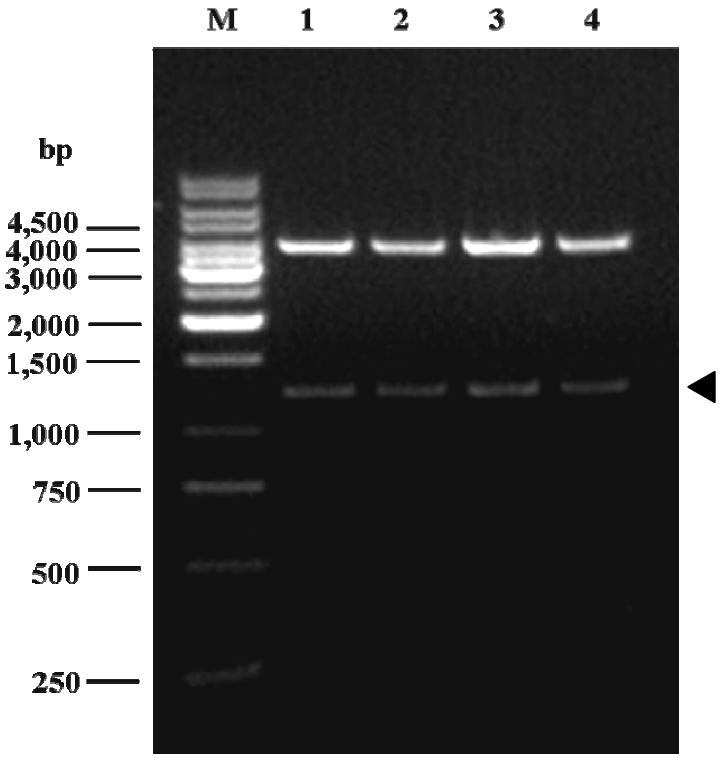

Figure 32 Digestion of purified recombinant pET20b(+)/FgLGMN-1 and -2 plasmids with *Hin*d III and *Xho* I restriction endonucleases. Lane M: 500 ng of 1 Kb DNA marker (Fermentas Life Sciences, Vilnius, Lithuania), lane 1 and 2: digested recombinant pET20b(+)/ FgLGMN-1, lane 3 and 4: digested recombinant pET20b(+)/ FgLGMN-2. Arrow head indicates an expected fragment size and the positions of the 1 Kb DNA standard fragments are indicated at the left side. Lane M: 500 ng of 1 Kb DNA marker (Fermentas Life Sciences, Vilnius, Lithuania).

4.2 Expression of recombinant FgLGMN proteins in a prokaryotic expression system (pET20b(+)/BL21(DE3)pLysS) and purification

The bacterially expressed recombinant proteins had a mass of approximately 49 kDa for FgLGMN-1 and 47 kDa for FgLGMN-2 which are expected molecular masses for fusion proteins including prokaryotic signal peptide molecular mass, predicted molecular mass of legumains and 6× His-tag molecular mass. Analysis of target protein solubility showed that the two recombinant FgLGMNs were formed in the insoluble material (Figure 33) and time-course analysis showed that two recombinant proteins were highly expressed since an hour after induction and were stable until four hours (Figures 34 and 35). The expression results suggested that two novel legumains from *F. gigantica* can be expressed in the pET20b(+)/BL21(DE3)pLysS prokaryotic expression system. On the other hand, other prokaryote expression systems, such as pQE30/M15, were used to establish expression of the two FgLGMNs but this system was found not be suitable.

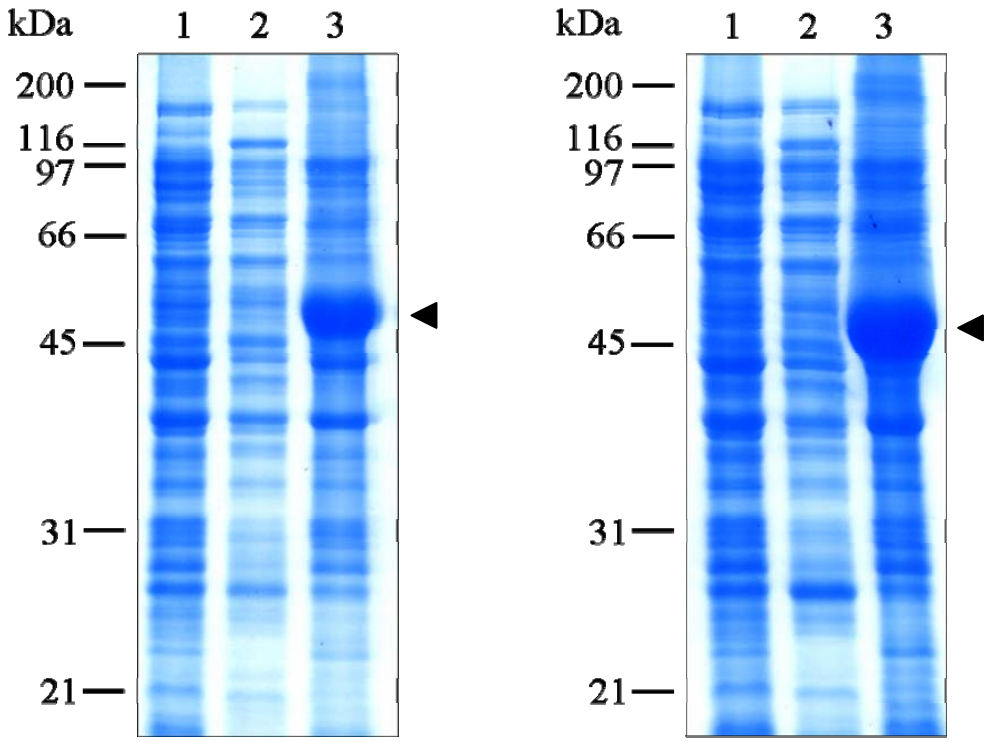

Figure 33 Analysis of target protein solubility by SDS-PAGE showed that *E. coli* BL21(DE3)pLysS transformants carrying pET20b(+)/FgLGMN-1 or -2 express recombinant proteins which form an insoluble product. Figure A: expression of recombinant FgLGMN-1. Figure B: expression of recombinant FgLGMN-2. In both figures, lane 1: crude non-induced, lane 2: induced soluble fraction, lane 3: induced insoluble fraction. The positions of broad range protein standard (Bio-Rad, USA) are indicated at the left side.

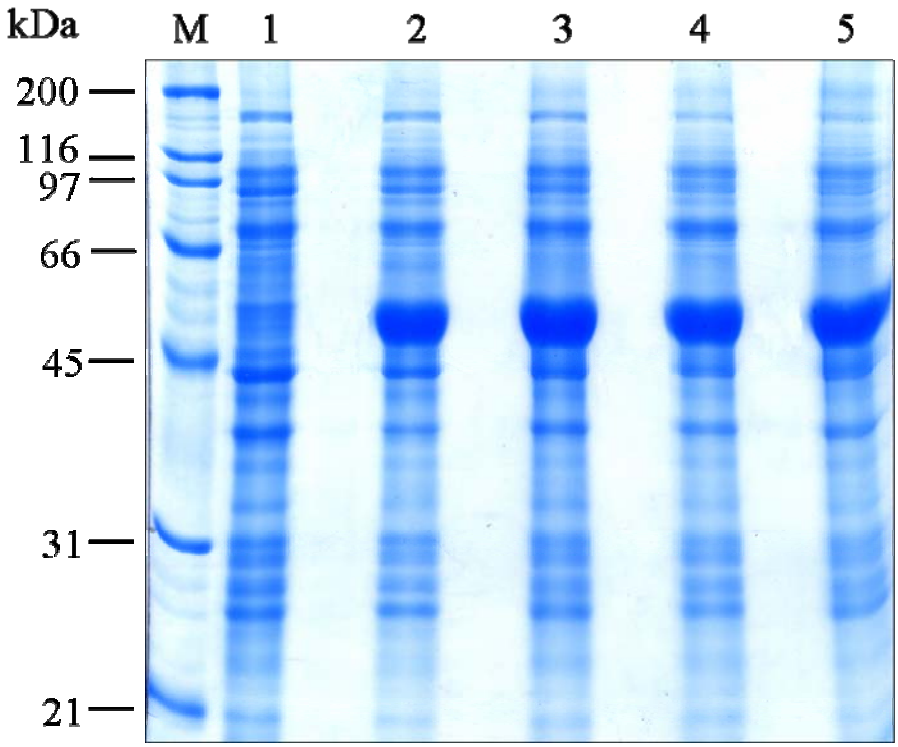

Figure 34 SDS-PAGE of time-course analysis showing the kinetics of expression of recombinant FgLGMN-1 proteins by *E. coli* BL21(DE3)pLysS transformants carrying pET20b(+)/ FgLGMN-1. Lane M: broad range protein standard (Bio-Rad, USA), lane 1: 0 hour (non-induced), lane 2: induced 1 hour, lane 3: induced 2 hours, lane 4: induced 3 hours, lane 5: induced 4 hours. The positions of broad range protein standard are indicated at the left side.

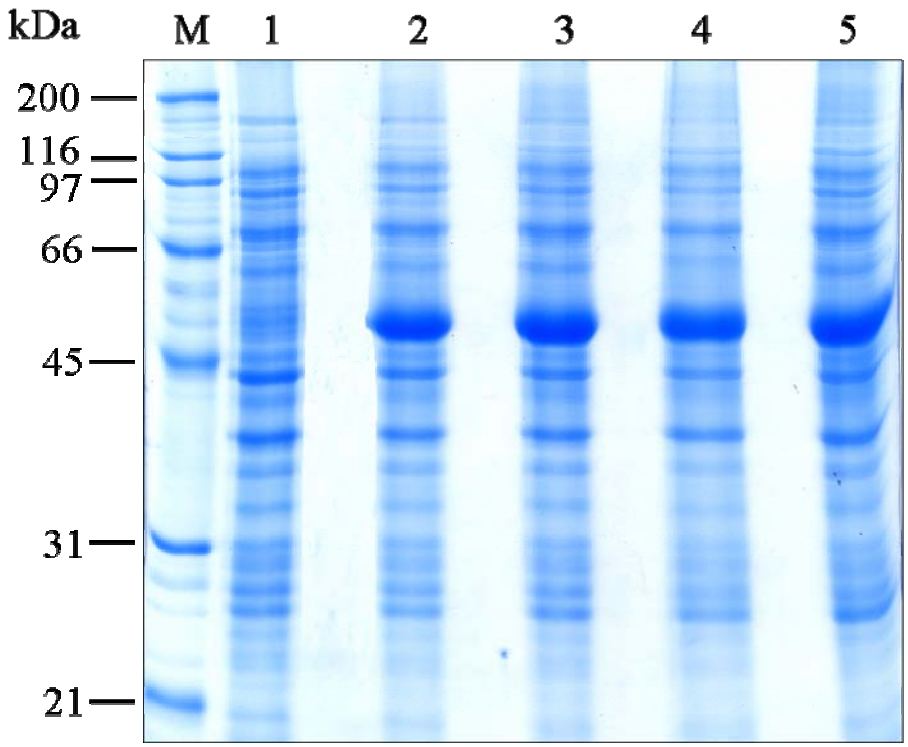

Figure 35 SDS-PAGE of time-course analysis showing the kinetics of expression of recombinant FgLGMN-2 proteins by *E. coli* BL21(DE3)pLysS transformants carrying pET20b(+)/ FgLGMN-2. Lane M: broad range protein standard (Bio-Rad, USA), lane 1: 0 hour (non-induced), lane 2: induced 1 hour, lane 3: induced 2 hours, lane 4: induced 3 hours, lane 5: induced 4 hours. The positions of broad range protein standard are indicated at the left side.

Recombinant FgLGMN-1 and -2 proteins were purified by using Ni-NTA affinity-chromatography (Qiagen, Germany) under denaturing conditions containing 8 M Urea and analyzed by 12% SDS-PAGE. The eluted fractions of recombinant FgLGMN-1 protein (Figure 36, lane 6 to 13) and recombinant FgLGMN-2 protein (Figure 37, lane 6 to 13) were pooled together and dialyzed against 0.01 M PBS, pH 7.2 to eliminate urea. The white slurry pellet appeared after decreasing of urea concentration and the recombinant proteins pellets were obtained by centrifugation. The pellet was dissolved in SDS-PAGE sample buffer and analyzed by 12% SDS-PAGE (Figure 38). Consequently, recombinant proteins were subjected to immunize experimental animals for production of polyclonal antiserum against recombinant proteins.

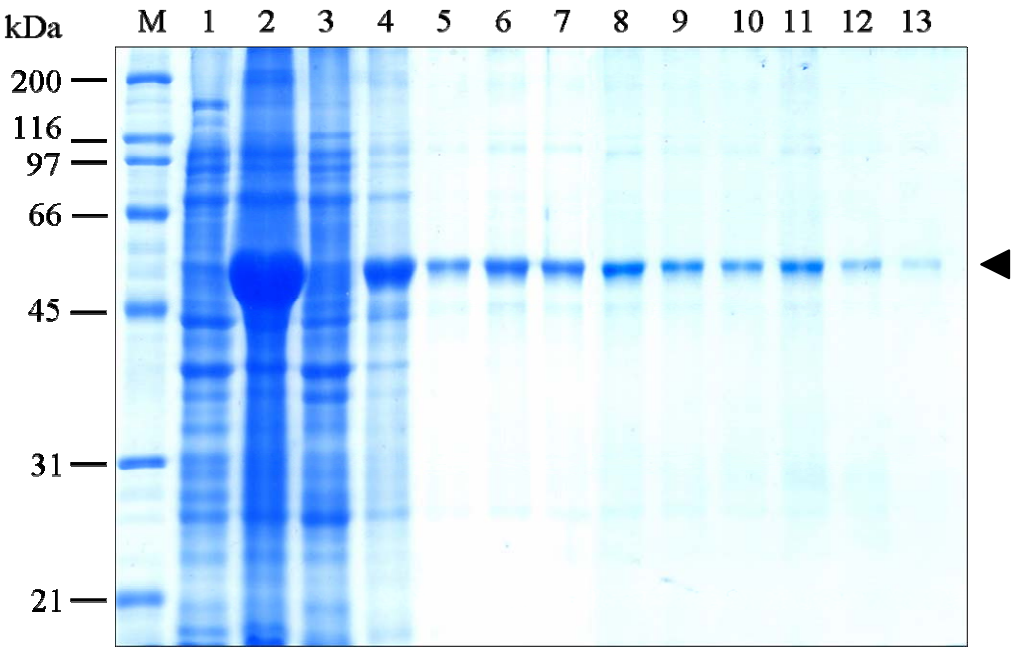

Figure 36 SDS-PAGE of recombinant FgLGMN-1, purified under denaturing conditions by Ni-NTA affinity chromatography. Lane M: broad range protein standard marker, lane 1: non-induced clear lysate, lane 2: induced clear lysate, lane 3: flow through, lane 4 and 5: wash fraction, lane 6 to 13: elution fraction. Recombinant FgLGMN-1 expressed in predominant bands at 49 kDa (arrowhead). The positions of broad range protein standard (Bio-Rad, USA) are indicated at the left side.

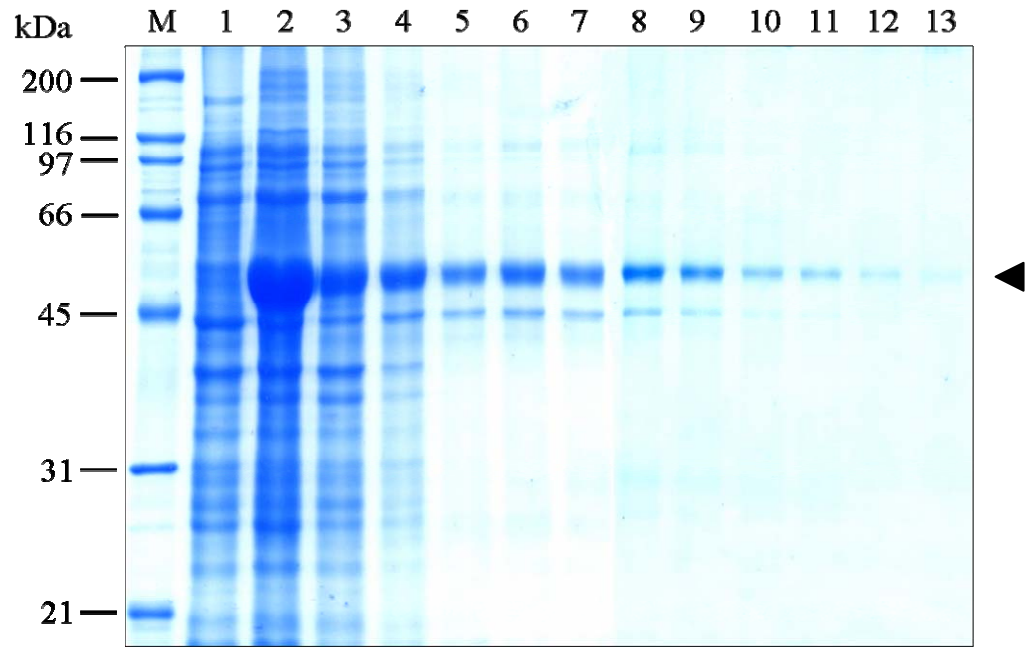

Figure 37 SDS-PAGE of recombinant FgLGMN-2, purified under denaturing conditions by Ni-NTA affinity chromatography. Lane M: broad range protein standard marker, lane 1: non-induced clear lysate, lane 2: induced clear lysate, lane 3: flow through, lane 4 and 5: wash fraction, lane 6 to 13: elution fraction. Recombinant FgLGMN-2 expressed in predominant bands at 47 kDa (arrowhead). The positions of broad range protein standard are indicated at the left side.

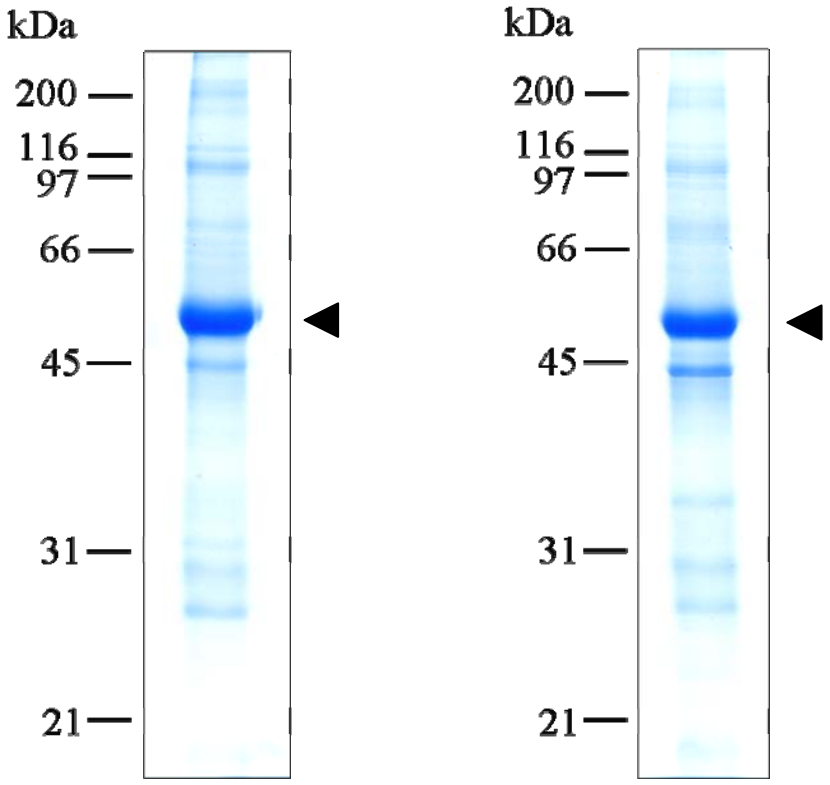

Figure 38 SDS-PAGE analysis of purified and dialysed recombinant proteins. The predominant purified recombinant FgLGMN-1 (Figure A) at 49 kDa and FgLGMN-2 (Figure B) at 47 kDa. The co-purification proteins were observed that represented contaminating bacterial proteins and may be complex or truncated rFgLGMNs.

4.3 Production of polyclonal antibodies against the recombinant FgLGMN-1 and FgLGMN-2 proteins

Two female New Zealand white rabbits were immunized with recombinantFgLGMN-1 and -2 proteins. Blood from rabbits was extracted before immunization and used as negative control. Two weeks after the second boost, blood was collected and immune sera were obtained sera for characterization of recombinant and native proteins and immunohistochemistry. The characterization of proteins and immunohistochemistry are described further on.

5. Characterization of FgLGMN-1 and FgLGMN-2 proteins

5.1 Detection of immune response against recombinant FgLGMNs in *F. gigantica*-infected mice

BALB/c mice were infected with infective stage (metacercariae) of *F. gigantica* and blood was collected at different weeks after infection (WAI). Specific antibody-mediated immune response in infected animals was detected by interaction infected mouse sera (0, 1, 2, 4 and 6 WAI) with recombinant FgLGMN-1 and -2 proteins according to western blot analysis procedure. The positive predominant band at a molecular weight of 49 kDa that is the size of expressed FgLGMN-1 was detected at 4 WAI and 6 WAI (Figure 39). Consistently, the purified FgLGMN-2 recombinant protein was detected at the molecular weight of 47 kDa at 4 WAI and 6 WAI (Figure 40). The evaluation of immune response in mouse could not be prolonged until parasite full development to the adult stage because mouse is an indefinite host for *F. gigantica* and more severe complications cause the death of experimental animals. Some of them died since 4 WAI and mostly died 6 WAI.

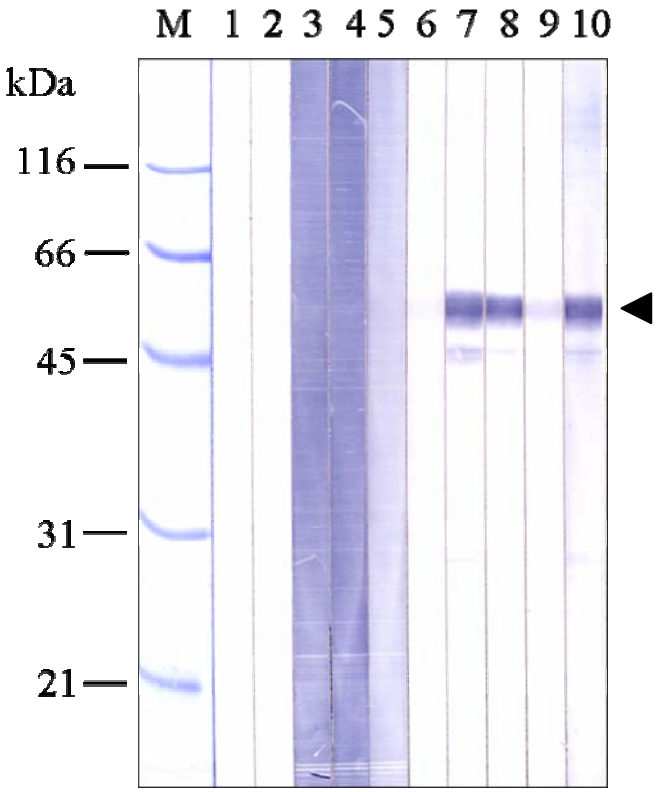

Figure 39 Western blot analysis of recombinant FgLGMN-1 reacted with *F. gigantica* infected mouse sera obtained at different weeks after infection. rFgLGMN-1 reacted with; week 0 (lanes 1 and 2), week 1 (lanes 3 and 4), week 2 (lanes 5and 6), week 4 (lanes 7 and 8), week 6 (lanes 9 and 10) and the arrowhead indicates reacted rFgLGMN-1.

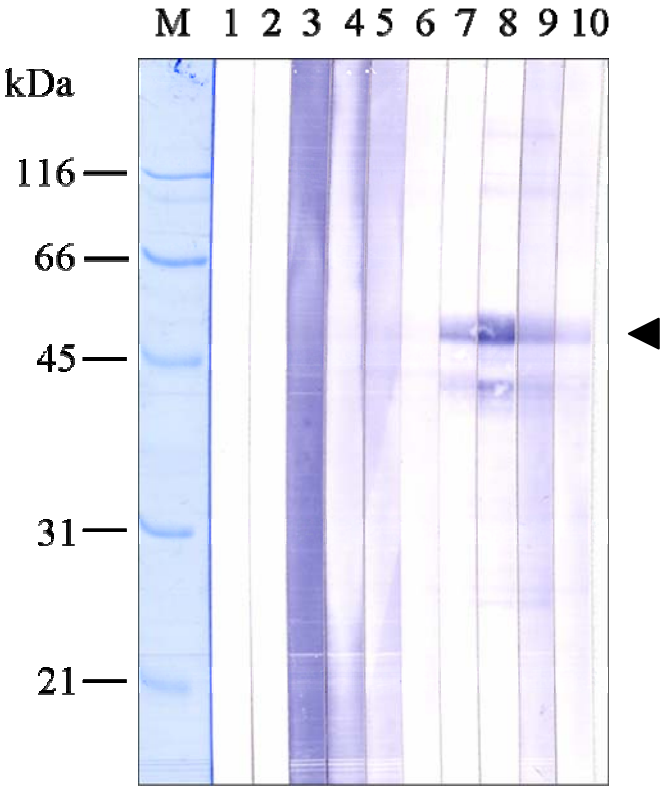

Figure 40 Western blot analysis of recombinant FgLGMN-2 reacted with *F. gigantica* infected mouse sera obtained at different weeks after infection. rFgLGMN-2 reacted with; week 0 (lanes 1 and 2), week 1 (lanes 3 and 4), week 2 (lanes 5and 6), week 4 (lanes 7 and 8), week 6 (lanes 9 and 10) and the arrowhead indicates reacted rFgLGMN-2.

5.2 Immunological characterization of recombinant FgLGMN and native proteins by using rabbit immune sera against recombinant proteins

Rabbit anti-rFgLGMNs polyclonal sera were used for characterization of recombinant and native proteins. Western blot analysis of recombinant proteins showed that anti-rFgLGMN-1 polyclonal serum detected rFgLGMN-1 but not rFgLGMN-2 protein (Figure 41A). Anti-rFgLGMN-2 polyclonal serum detected rFgLGMN-2 but not rFgLGMN-1 (Figure 41B). In crude parasite extracts, anti-rFgLGMN-1 detected native protein of a molecular mass of 40 kDa and anti-rFgLGMN-2 detected native protein of a molecular mass of 30 kDa (Figure 42). In contrast, polyclonal sera could not detect soluble FgLGMNs released in the excretory-secretory products. This experiment was performed both, in a colorimetric and chemiluminescent assay. Additionally, the quality of ESAg was determined by interaction with monoclonal Ab against *F. gigantica* Cathepsin L1, the major secretion product that exhibited the predominant positive bands at expected size of Cathepsin L1 (Figure 43).

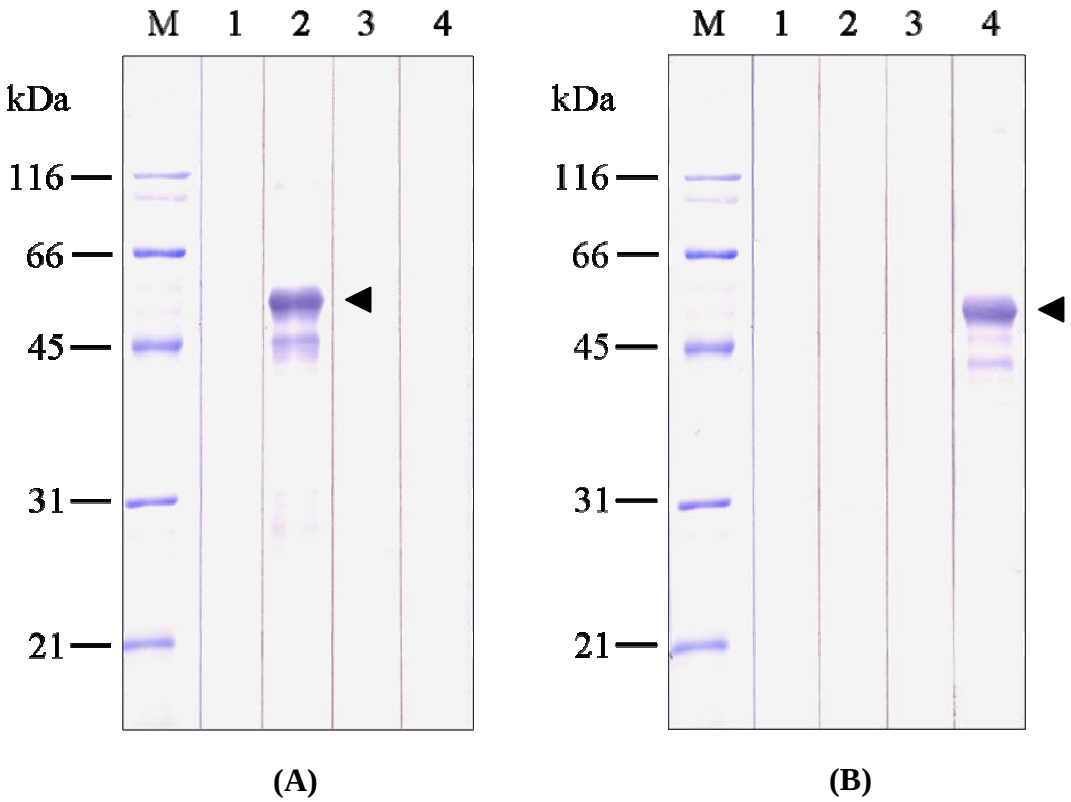

Figure 41 Immunoblot analysis of the reaction of FgLGMN-specific antibodies against the recombinant proteins and their cross-reaction. Figure A: detection of rFgLGMNs by rabbit anti-rFgLGMN-1 serum, lane 1: rFgLGMN-1 with control serum; lane 2: rFgLGMN-1 with anti-FgLGMN-1 serum; lane 3: rFgLGMN-2 with control serum; lane 4: rFgLGMN- 2 with anti-FgLGMN-1 serum. Figure B: detection of rFgLGMNs by rabbit anti-rFgLGMN-2 serum, lane 1: rFgLGMN-1 with control serum; lane 2: rFgLGMN-1 with anti-rFgLGMN-2 serum; lane 3: rFgLGMN-2 with control serum; lane 4: rFgLGMN-2 with anti-rFgLGMN-2 serum. Each rabbit anti-rFgLGMNs serum specifically detected the recombinant proteins and no cross-reaction appeared. The arrowhead indicates the reacted recombinant proteins and the positions of broad range protein standard are indicated at the left side.

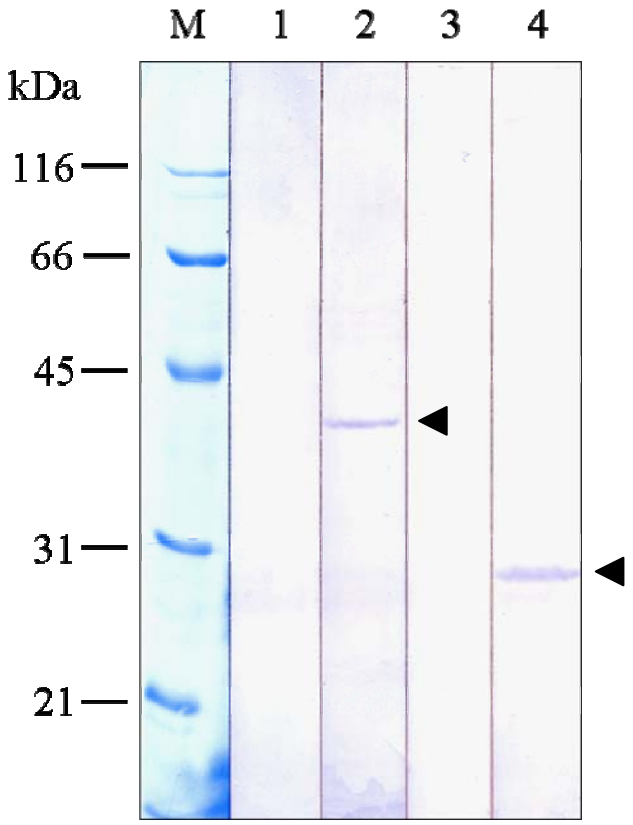

Figure 42 Immunoblot analysis of native proteins in crude adult parasite extracts with rabbit anti-rFgLGMN polyclonal sera indicated that rabbit anti-rFgLGMN-1 detected the native protein at the molecular size of 40 kDa and rabbit anti-rFgLGMN-2 at 30 kDa, lane 1: control serum; lane 2: anti-rFgLGMN-1; lane 3: control serum; lane 4: anti-rFgLGMN-2, lane M: broad range protein standard marker. The arrowhead indicates the reacted native proteins and the positions of broad range protein standard are indicated at the left side.

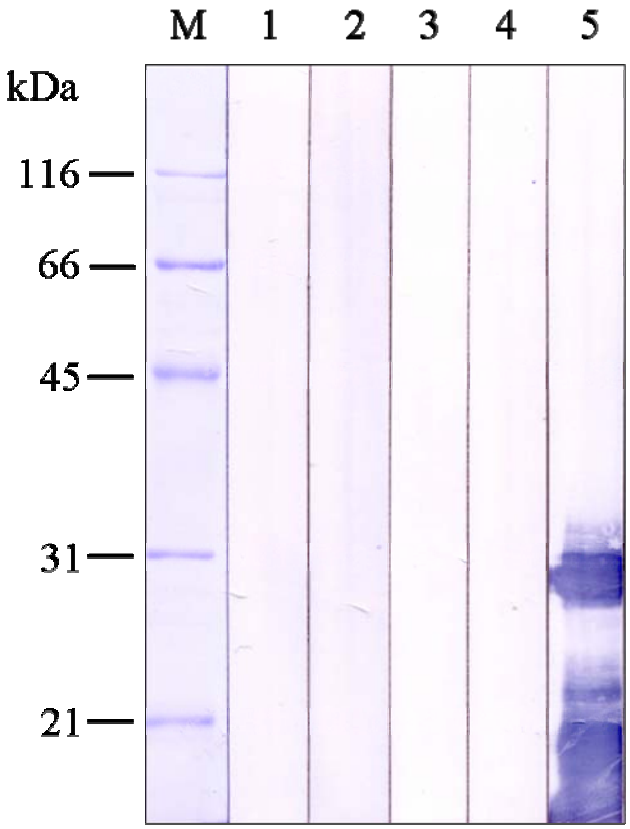

Figure 43 Immunoblot analysis of native proteins in excretory-secretory (ES) products prepared by *in vitro* culture of adult parasites. ES antigens reacted with rabbit anti-rFgLGMN polyclonal sera and the results showed that no proteins can be detected. The quality of ES antigens were determined by monoclonal Ab against FgCatL1, which showed a strong positive signal at 28-31 kDa (lane 5) that are expected size of *F. gigantica* cathepsin L1. Lane M: broad range protein standard marker (Bio-Rad, USA), lane 1: control serum; lane 2: anti-rFgLGMN-1; lane 3: control serum; lane 4: anti-rFgLGMN-2, lane 5: monoclonal Ab against FgCatL1. The positions of broad range protein standard are indicated at the left side.

5.3 N-glycosylation analysis of native FgLGMNs

The N-glycosylation of native proteins was determined by deglycosylation of native legumains with N-Glycosidase F (New England Biolabs® Inc., USA). The deglycosylated poteins and native proteins were size-separated on 12% SDS-PAGE (Figure 44) and transferred to PVDF membrane and western blot analysis with rabbit anti-rFgLGMNs polyclonal sera was done. The deglycosylated proteins were detected at the molecular mass of 40 kDa for FgLGMN-1 and 30 kDa for FgLGMN-2 that represent the molecular mass of native proteins (Figure 45). These results suggested that no N-glycosylation of *F. gigantica* legumains occurs.

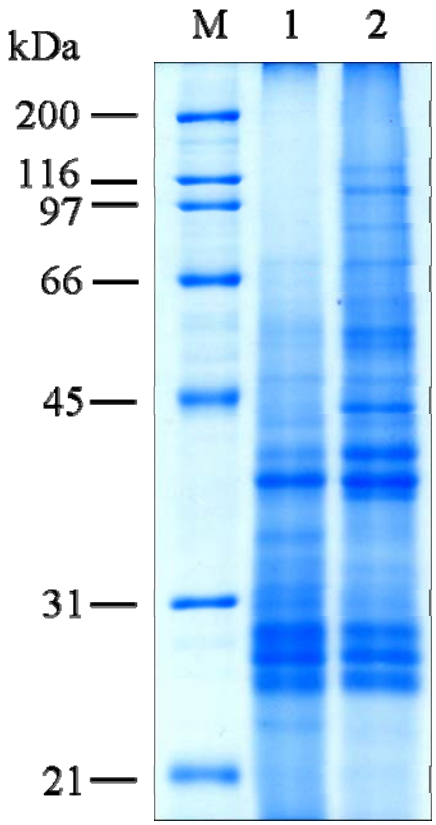

Figure 44 SDS-PAGE of crude parasite antigens (CWA) after N-deglycosylation. Lane M: broad range protein standard marker (Bio-Rad, USA), lane 1: normal CWA, lane 2: N-deglycosylated CWA. The positions of broad range protein standard are indicated at the left side.

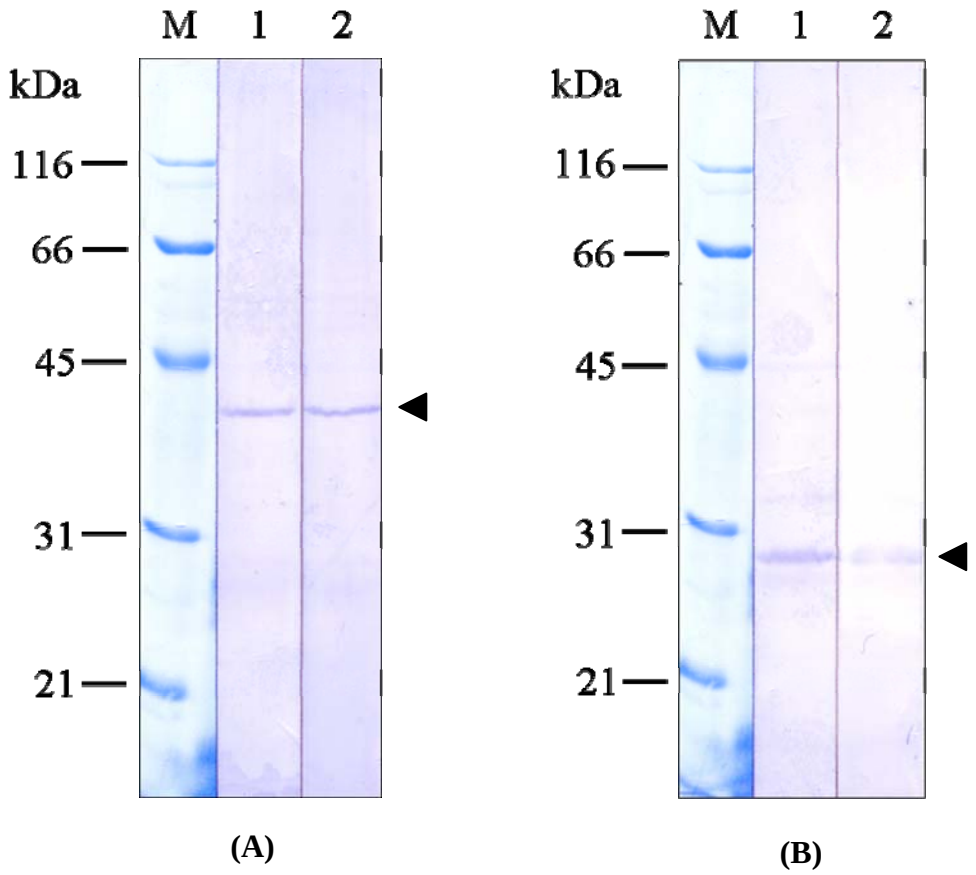

Figure 45 Immunoblot analysis of native FgLGMNs after N-deglycosylation showed that rabbit anti-rFgLGMN-1 detected N-deglycosylaed protein at a molecular size of 40 kDa (lane 1), the same as the native protein (lane 2) (Figure A). Consistently, rabbit anti-rFgLGMN-2 detected N-deglycosylated protein at a molecular size of 30 kDa (lane 1) the same as the native protein (lane 2) (Figure B). The results suggested that N-glycosylation processing might not take place in molecules of FgLGMN-1 and FgLGMN-2 proteins. The positions of broad range protein standard are indicated at the left side.

6. Immunolocalization of native proteins in tissues of 4-week old juvenile and adult parasites by using rabbit anti-rFgLGMNs polyclonal sera

Polyclonal rabbit anti-rFgLGMN-1 and -2 sera were used to analyze the anatomical localization of native LGMN-1 and -2 in tissue sections of 4-week old juvenile and adult *F. gigantica*. Tissue sections were incubated with anti-rFgLGMNs polyclonal sera. FgLGMN-1 and -2 were specifically expressed in gastrodermis tissue. The localization of FgLGMN-1 was detected in the gastrodermal epithelial cells that are distributed in cytoplasm and mostly in the large granules which are concentrated in the apical part of these cells of adult stage parasites (Figures 46A-D). In 4-week old juveniles, the localization of FgLGMN-1 was detected in the gastrodermis tissue as well (Figures 47A and B). Tissue sections that were incubated with (normal) control sera showed negative staining in adult and 4-week old juvenile parasites (Figures 46E and 47C).

The FgLGMN-2 was localized in the gastrodermal epithelial cells and contained in fine granules which accumulated in the microvilli (Figures 48A, B, C and E). In 4-week old juvenile parasite, the localization of FgLGMN-2 was detected in the gastrodermis tissue as well (Figures 49A and B). Tissue sections that were incubated with (normal) control sera showed negative staining in adult and 4-week old juvenile parasites (Figures 48D and 49C).

The immunohistochemistry results are consistent with *in situ* hybridization that indicated that two novel legumains of *F. gigantica* are gut-specific proteases.

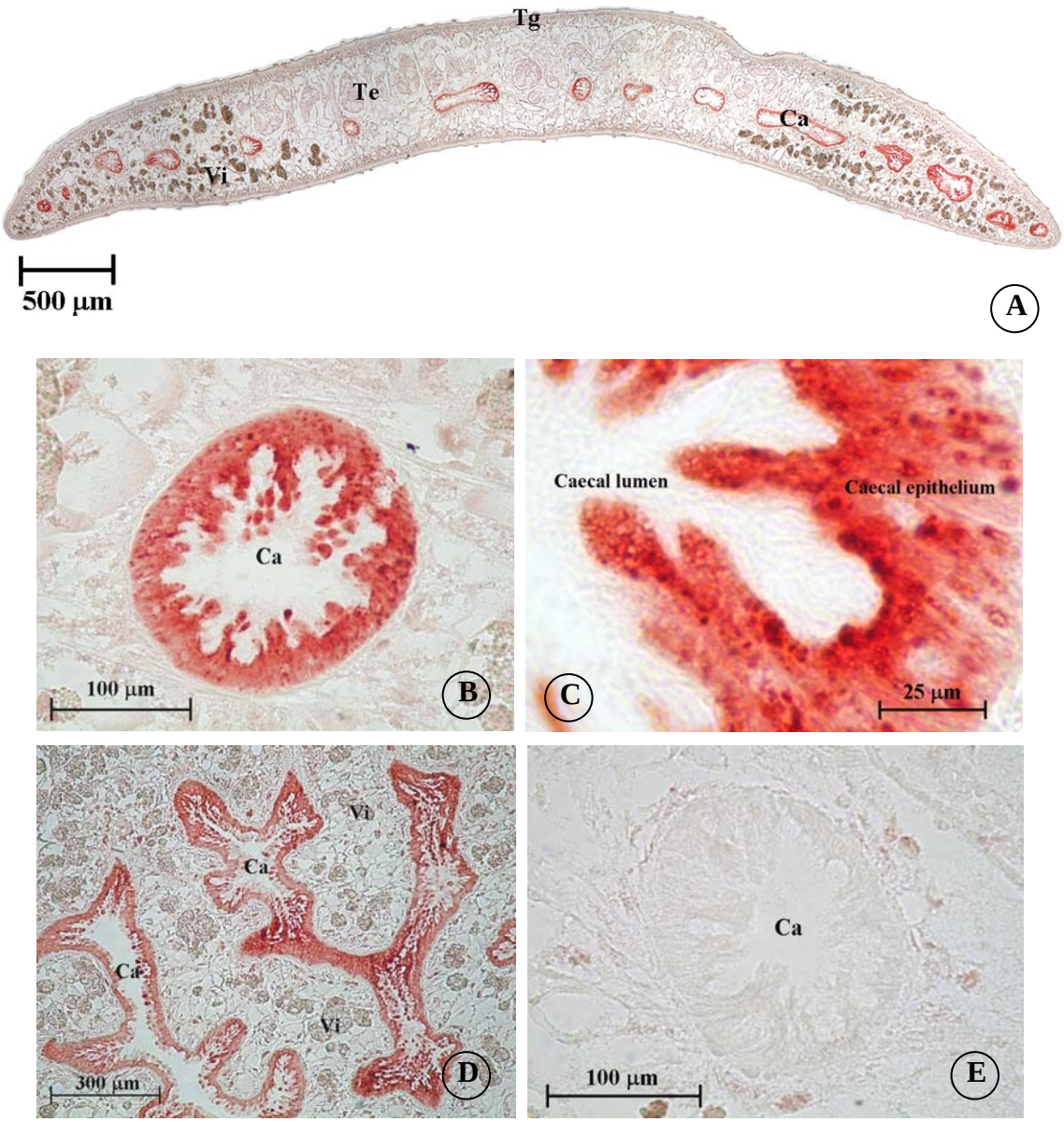

Figure 46 Immunohistolocalization of FgLGMN-1 in tissues of adult *F. gigantica*. The localization of expressed protein was detected by a rabbit anti-rFgLGMN-1 polyclonal serum. LGMN-1 is distributed in the gastrodermal epithelium with high concentration in large granules mainly localized to the marginal area of microvilli. A: whole cross-section of adult parasite. B: cross-section of adult at low magnification. C: adult, high magnification of the caecal epithelium. D: longitudinal section of adult parasite. E: negative control using the pre-immune serum. Ca: caecum; Te: Testis; Tg: tegument and Vi: vitelline gland

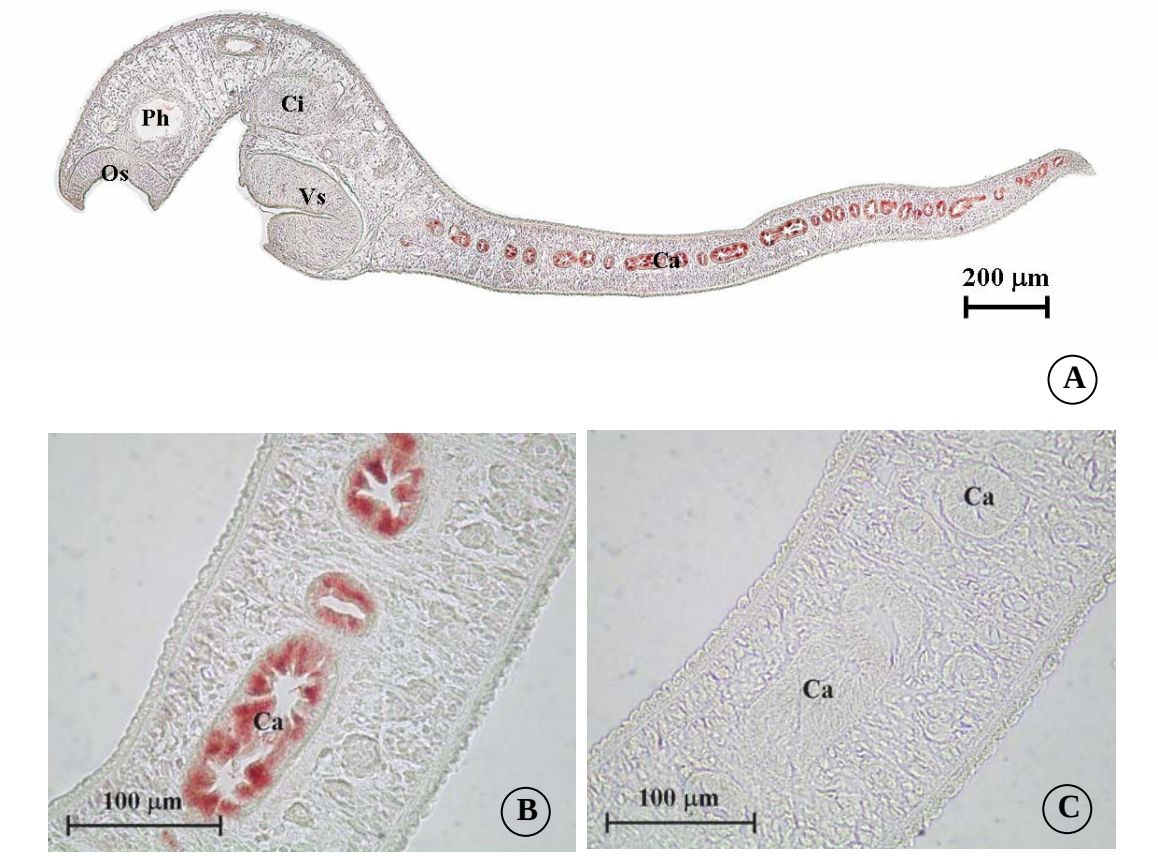

Figure 47 Immunohistolocalization of FgLGMN-1 in tissues of 4-week juveniles *F. gigantica*. The localization of expressed protein was detected by a rabbit anti-rFgLGMN-1 polyclonal serum. LGMN-1 is distributed in the gastrodermal epithelium localized to the marginal area of microvilli. A: full-length sagittal section of adult parasite. B: sagittal section at high magnification of 4-week juvenile. C: negative control using the pre-immune serum. Ca: caecum; Ci: cirrus porous; Os: oral sucker; Ph: pharynx and Vs: ventral sucker

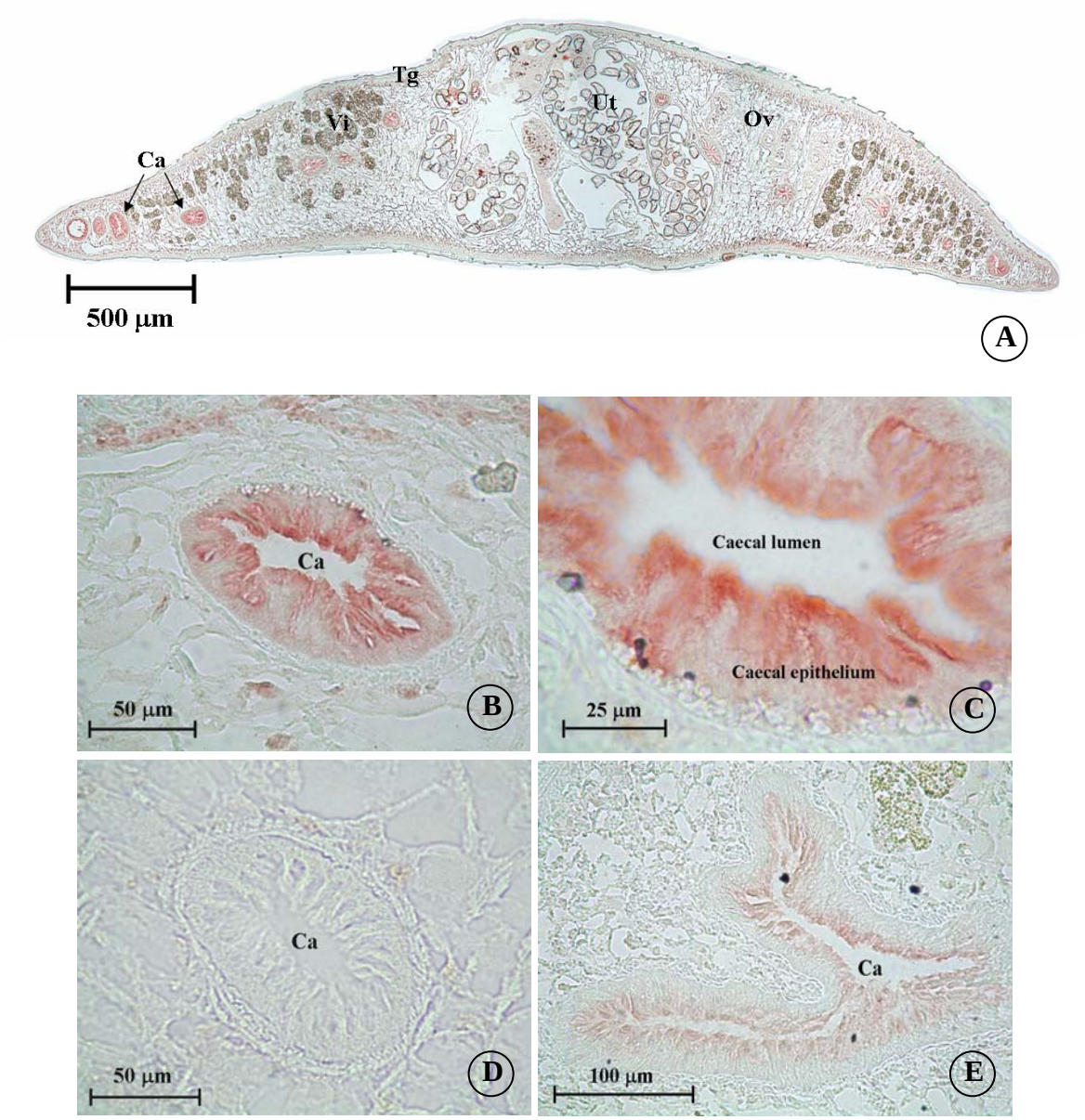

Figure 48 Immunohistolocalization of FgLGMN-2 in tissues of adult *F. gigantica*. The localization of expressed protein was detected by a rabbit anti-rFgLGMN-2 polyclonal serum. LGMN-2 is distributed in the gastrodermal epithelium in fine granules, localized at the marginal area of microvilli. A: whole cross-section of adult parasite. B: cross-section of adult at low magnification. C: adult, high magnification of the caecal epithelium. D: negative control using the pre-immune serum. E: longitudinal section of adult parasite. Ca: caecum; Ov: ovary; Tg: tegument; Ut: uterus and Vi: vitelline gland

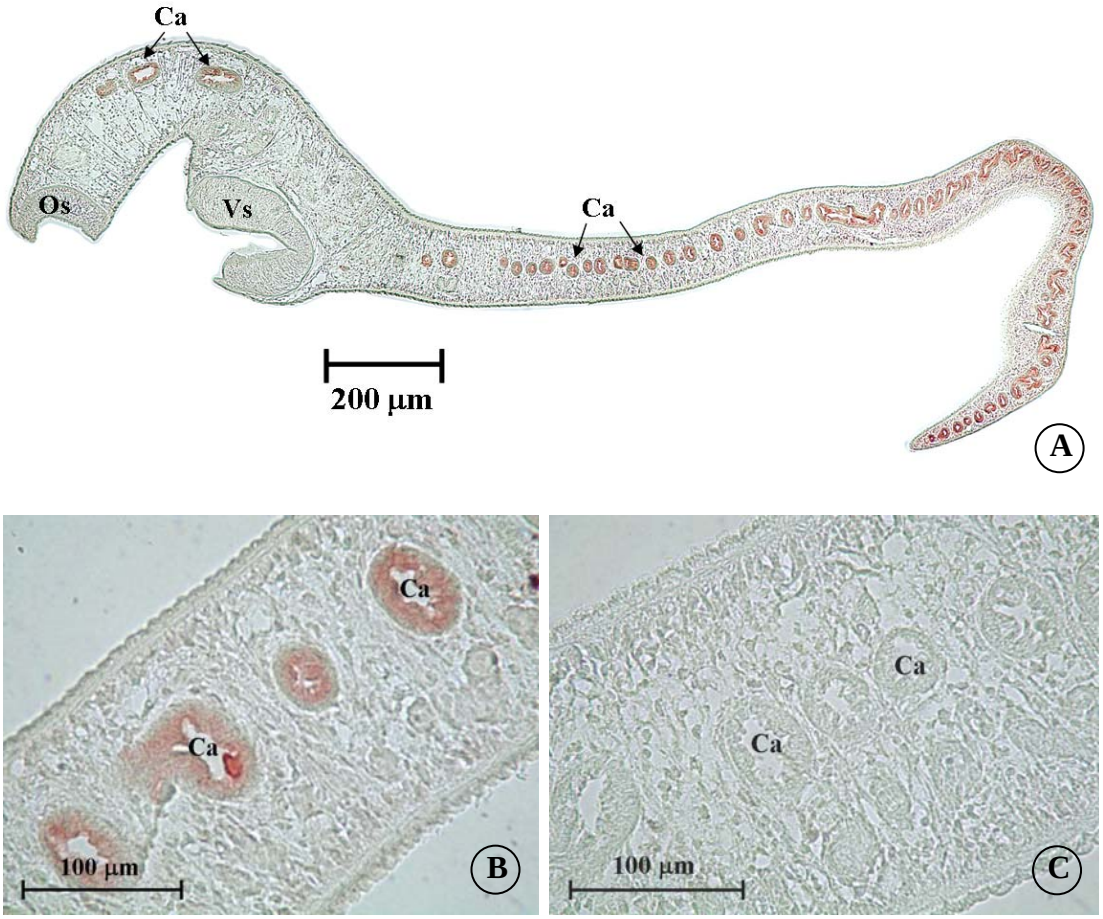

Figure 49 Immunohistolocalization of FgLGMN-2 in tissues of 4-week juvenile *F. gigantica*. The localization of expressed protein was detected by a rabbit anti-rFgLGMN-2 polyclonal serum. LGMN-2 distribute in the gastrodermal epithelium localized to the marginal area of microvilli. A: full-length sagittal section of adult parasite. B: sagittal section at high magnification of 4-week juvenile. C: negative control using the pre-immune serum. Ca: caecum; Os: oral sucker Vs: ventral sucker

7. Autocatalytic processing and functional assay of recombinant FgLGMN and native proteins

7.1 Autocatalytic processing and functional assay of recombinant FgLGMN proteins

Recombinant FgLGMN proteins were subjected to evaluate the autoactivation mechanism by exposure to pH value in range 4-7. Previous studies proposed that this mechanism is pH-dependent, especially in acidic pH. For the recombinant FgLGMN-1 protein, the autocatalytic processing appeared at pH 5 by slightly decreasing of 49 kDa by-product and generation of small amounts of 48 and 30 kDa autocatalytic products. At pH 4, the amount of autocatalytic products was increasing as counterpart to the decreasing amount of the original (Figure 50A). The autocatalytic mechanism was inhibited at higher pH (pH 6 and 7) and showed only the original product and no autocatalytic products (Figure 50A). In consistence to SDS-PAGE, the immunoblot of the autocatalytic products shows that anti-rFgLGMN-1 serum detects autocatalytic products of recombinant proteins when exposed to acidic pH (Figure 50B).

For recombinant FgLGMN-2 protein, the small amount of autocatalytic products at the size of approximately 46 kDa appeared when exposed to acidic pH (pH 5 and 4) (Figure 51A). The immunoblot was performed by probing with anti-FgLGMN-2 serum and confirmed the result of SDS-PAGE (Figure 51B).

After autocatalytic processing, recombinant proteins were incubated with a specific synthetic peptide substrate to legumains (Bz-Asn-pNA). Unfortunately, the autocatalytic proteins failed to hydrolyze the specific substrate like the negative control (boiled recombinant protein).

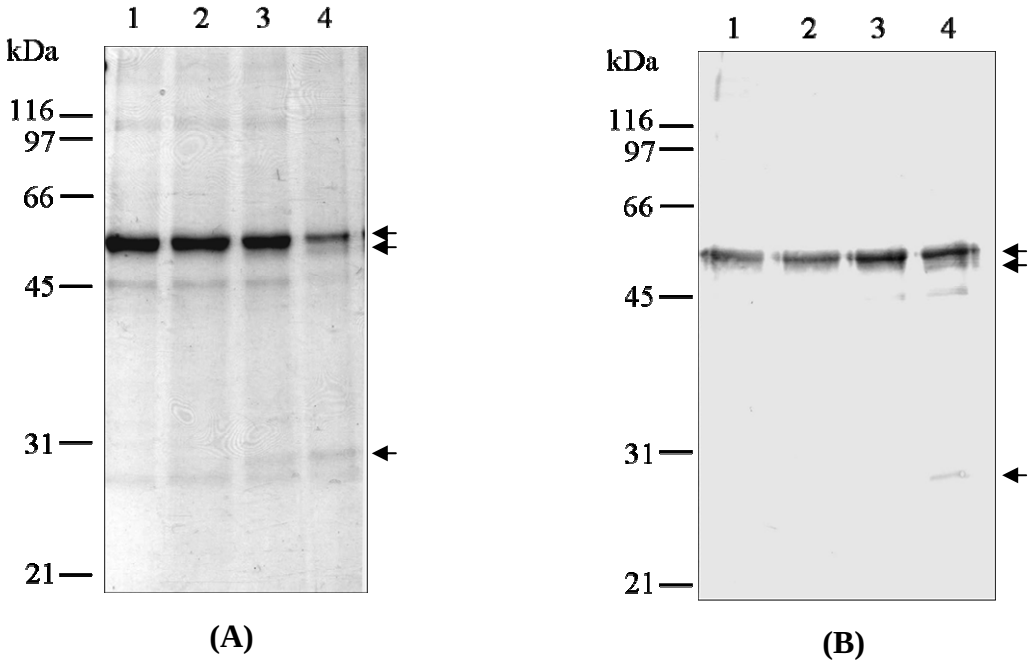

Figure 50 12% SDS-PAGE (A) and immunoblot (B) of products generated after autoprocessing of recombinant FgLGMN-1 that was exposed to different pH values; pH 7 (lane 1), pH 6 (lane 2), pH 5 (lane 3) and pH 4 (lane 4). The arrows indicate the original product (49 kDa) and autocatalytic products (48 and 30 kDa).

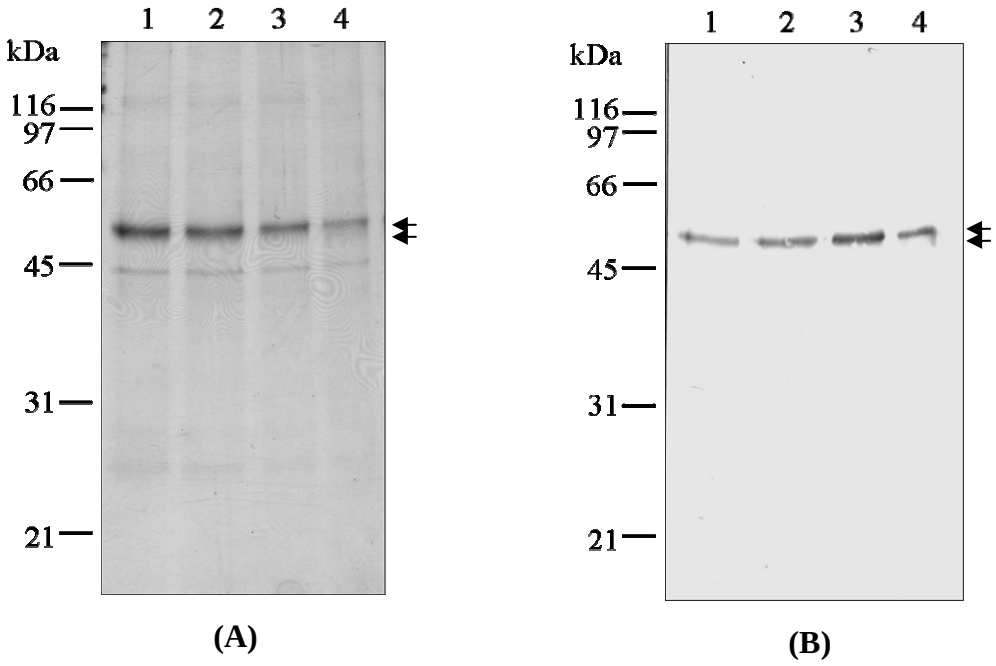

Figure 51 12%SDS-PAGE (A) and immunoblot (B) of products generated after autoprocessing of recombinant FgLGMN-2 that was exposed to different pH values; pH 7 (lane 1), pH 6 (lane 2), pH 5 (lane 3) and pH 4 (lane 4). The arrows indicate the original product (47 kDa) and autocatalytic products (46 kDa).

7.2 Legumain activity and inhibition sensitivity assays of adult *F. gigantica* antigens

The legumain activity assays were performed with crude worm extracts and excretory-secretory products from adult *F. gigantica*. A specific substrate of legumains was purchased from BACHEM (Switzerland) and used in this experiment. The crude parasite antigen was incubated with the Bz-Asn-pNA substrate and the released pNA was measured to calculate the legumain activity. The optical density (mOD) in the sample was significantly increased when compared to the negative control (boiled CWAg) ($p<0.05$) (Table 9 and Figure 52). The legumain activity was also determined for excretory-secretory products of adult *F. gigantica*. The release of pNA in ESAg could not be distinguished from the negative control (boiled ESAg) ($p>0.05$) (Table 9 and Figure 52). This finding was consistent with the immunoblot of ESAg in which that no protein bands were detected with rabbit anti-rFgLMNs. These results suggested that legumain might not be secreted by cultured adult *F. gigantica*.

The inhibition profile of legumain activity was analyzed in CWAg. The activity was partially inhibited by PMSF which showed a remaining specific activity of 56%. The activity of legumain was reduced to 6% in the presence of IAA. With EDTA, the activity slightly decreased to 94% which showed the chelating agent has less effect on inhibition of legumain activity. The proteases inhibitors cocktail (PMSF, IAA and EDTA) decreased legumain activity to 3%. Enzyme activity in the presence of these inhibitors was expressed relative to the control set at 100% relative activity (Table 10 and Figure 53).

Table 9 Legumain activity in crude worm extracts and excretory-secretory products of adult *F. gigantica* determined by using synthetic peptide substrate Bz-Asn-pNA after incubation for 1 hour at pH 5.4 in the presence of 1 mM DTT. Boiled antigens were used as negative control.

Crude adult *F. gigantica* extracts	Legumain activity (total pNA released mOD_{405}; n=3)
Crude worm extracts (CWAg)	46.67 ± 7.024
Boiled crude worm extracts (b_CWAg)	0.00 ± 0.000
Excretory-secretory products (ESAg)	2.67 ± 1.528
Boiled excretory-secretory products (b_ESAg)	1.00 ± 1.000

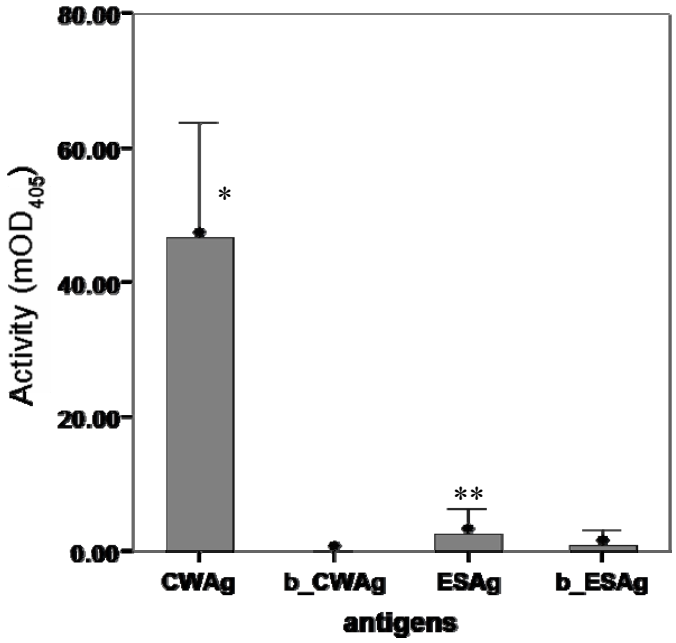

Figure 52 Legumain activity in adult parasite extracts. Crude worm extracts and excretory-secretory products of adult *F. gigantica* were incubated with Bz-Asn-pNA for 1 hour at pH 5.4 in the presence of 1 mM DTT. The activity was measured as mOD and boiled antigen was used as a negative control. The following abbreviations represent types of antigen; CWAg: crude worm extract, b_CWAg: boiled crude worm extract, ESAg: excretory-secretory products, b_ESAg: boiled excretory-secretory products. The statistical analysis between sample and negative groups was analyzed by the Man-Whitney test at 95% confidential limit; *: $p<0.05$, **: $p>0.05$

Table 10 Comparison of the effects of various protease inhibitors on the legumain activity of crude parasite extract. Enzyme activity in the presence of various compounds is expressed relative to the control set at 100%.

Inhibitors	Legumain activity (total pNA released mOD; n=3)	Relative activity (%)
control	34.00 ± 3.60	100
2mM phenylmethylsulfonyl fluoride (PMSF)	19.33 ± 2.51	56
5 mM iodoacetamide (IAA)	2.33 ± 3.21	6
1 mM ethylenediaminetetraacetate (EDTA)	32.00 ± 2.31	94
Cocktail (2 mM PMSF, 5 mM IAA and 1 mM EDTA; CT)	0.67 ± 0.58	3

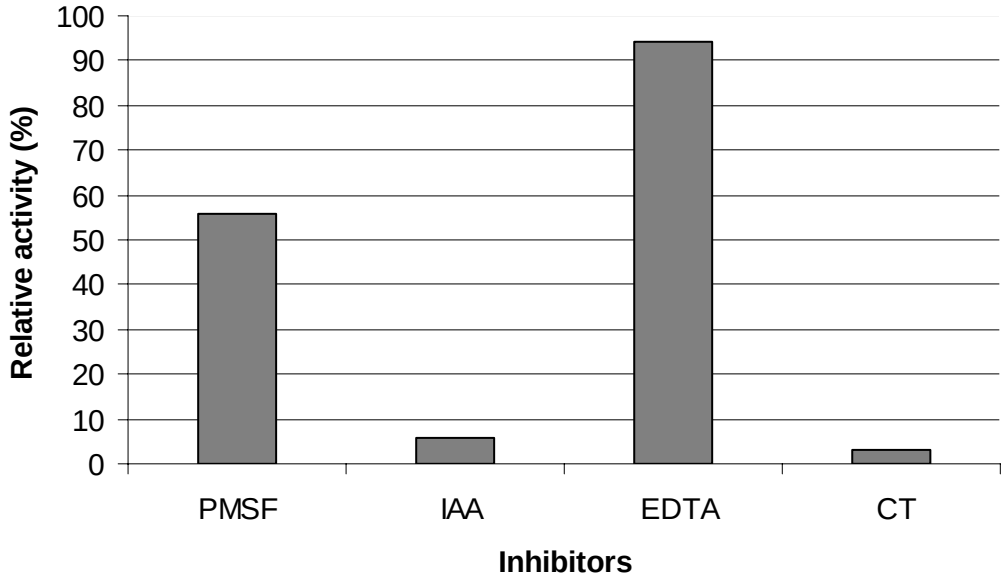

Figure 53 Comparison of the effect of various protease inhibitors on the legumain activity of crude parasite extracts. Enzyme activity in the presence of various compounds is expressed relative to the control set at 100%. Each inhibitor was added to each reaction tube to final concentration: 2 mM PMSF, 5 mM IAA, 1 mM EDTA and cocktail (2 mM PMSF, 5 mM IAA and 1 mM EDTA; CT).